EFFECTS OF INDUCTION HEATING PARAMETERS ON FORGING BILLET
TEMPERATURE

A THESIS SUBMITTED TO
THE GRADUATE SCHOOL OF NATURAL AND APPLIED SCIENCES
OF
MIDDLE EAST TECHNICAL UNIVERSITY

BY

İLKER DURUKAN

IN PARTIAL FULFILLMENT OF THE REQUIREMENTS
FOR
THE DEGREE OF MASTER OF SCIENCE
IN
MECHANICAL ENGINEERING

SEPTEMBER 2007

Approval of the thesis:

EFFECTS OF INDUCTION HEATING PARAMETERS ON FORGING BILLET TEMPERATURE

submitted by **İLKER DURUKAN** in partial fulfillment of the requirements for the degree of **Master of Science in Mechanical Engineering Department, Middle East Technical University** by,

Prof. Dr. Canan Özgen
Dean, Graduate School of **Natural and Applied Sciences**   _____

Prof. Dr. S. Kemal İder
Head of Department, **Mechanical Engineering**   _____

Prof. Dr. Mustafa İlhan Gökler
Supervisor, **Mechanical Engineering, METU**   _____

Prof. Dr. Haluk Darendeliler
Co-supervisor, **Mechanical Engineering, METU**   _____

Examining Committee Members:

Prof. Dr. Haluk Darendeliler
Mechanical Engineering, METU   _____

Prof. Dr. Mustafa İlhan Gökler
Mechanical Engineering, METU   _____

Assoc. Prof. Dr. Cemil Yamalı
Mechanical Engineering, METU   _____

Asst. Prof. Dr. İlker Tarı
Mechanical Engineering, METU   _____

Prof. Dr. Can Çoğun
Mechanical Engineering, Gazi University   _____

Date: _____

I hereby declare that all information in this document has been obtained and presented in accordance with academic rules and ethical conduct. I also declare that, as required by these rules and conduct, I have fully cited and referenced all material and results that are not original to this work.

Name, Last Name: İlker DURUKAN

Signature   :

ABSTRACT

EFFECTS OF INDUCTION HEATING PARAMETERS ON FORGING BILLET TEMPERATURE

DURUKAN, İlker

M.Sc., Department of Mechanical Engineering

Supervisor: Prof. Dr. Mustafa İlhan GÖKLER

Co-Supervisor: Prof. Dr. Haluk Darendeliler

September 2007, 73 Pages

Induction heating is one of the efficient and modern technique for heating raw materials for hot forging process. The induction heating furnaces use electro-magnetic field to transfer energy to the metal workpiece and heat is generated inside the material. The magnetic field can be provided by using induction coil. The power supplied to induction coil, the moving speed of the billet that is called conveyor speed and the coil box hole diameter are the factors affecting the resultant temperature of the heated billet.

In this study, AISI 1045 type steel billets with a diameter of Ø 30 mm and length of 100 mm have been heated in a particular induction heater. During heating, effects of different levels of power, conveyor speed and the coil boxes with different hole diameters are investigated. The 125 KW 3000 Hz induction heater which is available in METU-BILTIR Research and Application Center Forging Laboratory is used in experiments. The heating experiments are designed according to 2^3 Factorial Design of Experiment Method. Multiple linear regression technique is used to derive a mathematical formula to predict the temperature of the heated billet. A good correlation between the measured temperatures that are the results of different sets of induction heating parameters and the predicted temperatures that are calculated by using temperature prediction formula has been observed.

Keywords: Induction Heating, Hot Forging, Induction Coil Box, Design of Experiment, Linear Regression Technique

ÖZ

İNDÜKSİYONLA ISITMA DEĞİŞKENLERİNİN DÖVME ÇUBUK SICAKLIĞINA ETKİLERİ

DURUKAN, İlker

Yüksek Lisans, Makina Mühendisliği Bölümü

Tez Yöneticisi: Prof. Dr. Mustafa İlhan GÖKLER

Ortak Tez Yöneticisi: Prof. Dr. Haluk Darendeliler

Eylül 2007, 73 Sayfa

İndüksiyonla ısıtma, sıcak dövme işlemi için hammalzemenin ısıtılmasında kullanılan verimli ve çagdaş bir tekniktir. İndüksiyonla ısıtma yapan fırınlar elektro-manyetik alanı kullanarak enerjiyi metal iş parçasına aktarırlar ve ısı malzemenin içinde oluşur. Manyetik alan, indüksiyon bobini kulanımı ile sağlanır. İndüksiyon bobinine sağlanan güç, taşıyıcı hızı olarak adlandırılan dövülecek çubuk ilerleme hızı ve indüksiyon bobin kutusu delik çapı, ısıtılan çubuğun son sıcaklığını etkileyen değişkenlerdir.

Bu çalışmada, AISI 1045 tip, çapı Ø30 mm ve boyu 100 mm olan çelik çubuklar bellirli bir indüksiyon fırınında ısıtılmışlardır. Isıtma sırasında, farklı güç, taşıyıcı hızı ve indüksiyon bobin kutu çaplarının etkisi incelenmiştir. Deneylerde ODTU-BİLTİR Araştırma ve Uygulama Dövme Laboratuvarıda bulunan 125 KW 3000 Hz indüksiyon ısıtısıcı kullanılmıştır. Isıtma deneyleri 2^3 Faktöriyel Deney Tasarım Methoduna göre yapılmıştır. Çoklu doğrusal regresyon tekniği kullanılarak ısıtılan çubukların sıcaklığını tahmin etmeye yönelik matematiksel bir denklem geliştirilmiştir. Farklı ısıtma parametreleri sonucu ölçülen sıcaklık değerleri ile matematiksel denklemden elde edilen sıcaklık değerleri karşılaştırılmasında iyi bir uyum gözlenmiştir.

Anahtar Sözcükler: İndüksiyonla Isıtma, Sıcak Dövme, İndüksiyon Bobini, Deney Tasarım Methodu, Doğrusal Regresyon Teknigi

To My Family

ACKNOWLEDGEMENTS

TABLE OF CONTENTS

LIST OF TABLES

LIST OF FIGURES

CHAPTER 1

INTRODUCTION

Induction heating is used in numerous applications in the metal working industry. When there is need to heat metal, the controlling of the heat transfer appears as a problem. Since, the induction heating has advantage of controlled energy transfer; it became popular in the metal working industry. Induction heating systems can transfer intensive energy very rapidly to the workpiece in a controlling manner. For this reason it is used in high energy need applications like melting of metal for casting and high temperature heating of billet for forging, extrusion or similar types of metal forming applications. Other utilization areas are the precise heating applications like surface hardening, annealing or sintering. In addition, it can be used special application like welding operations joining, brazing, bonding etc. Some industrial applications of the induction heating is shown on the Table 1.1

Table 1.1 Industrial Applications of Induction Heating [1]

Induction Melting	Induction Welding	Special applications
	-Induction brazing -Induction soldering	-Shrink fitting -Cap sealing
Induction Heating -Billet and bar heating -Strip and plate heating -Wire and cable heating -Tube and pipe heating	**Heat Treatment** -Hardening -Tempering -Annealing -Normalizing -Sintering -Carbide tipping	-Banding -Heat staking metal to plastic -Hot material testing -Sealing metal to glass

1.1 Hot Forging Application of the Induction Heating

Induction heating is widely employed in forging industry to heat billet that is to be forged in hot. In the steel working industry, hot forging steels are heated to temperatures around 1000 ^{o}C-1250 ^{o}C according to carbon content and the alloying elements [2]. The hot forging process requires high temperature heating of billet uniformly both along the cross sectional side and traverse side of the billet. Generally the initial temperature of the billet is in the room temperature and it is required to heat above the recrystallization temperature for hot forging process.

There are various ways to heat metal in hot forging including the induction heating, gas fired furnace, oil fired furnace, infrared heater and the electrical resistance heater. Induction heating has various advantages over the other methods of heating in hot forging. First of all, induction heating systems create high heat intensity very quickly at defined part of the metal. Additionally, induction heating systems are fast starting systems, since these systems do not need preheating time as in the furnace heating. Also, heating time is incompatibly short against the other methods. Compared to the gas and oil furnace heating, controlling and repeating the same heating condition for different time is easier to achieve. Automation can be applied to the induction heating systems. It will require minimum shop floor space. Induction heating is also more energy efficient and more environmental friendly. There will not be any harmful combustion emission to the environment as in the gas and oil furnace heating. Further more the gas fired furnaces result with poor surface quality due to scale formation. The induction heating provides significant reduction in scale formation and decarburization on the heated billet.

1.2 Scale Formation

A thin layer of iron oxide called scale covers the surface of the hot forging steels, which is caused by contact of the hot steel with air. The oxidation of the steel begins at about 200 °C; and serious scaling, where substantial material may be lost and oxidized material spells off the surface of the material, does not begin until the material reached about 850°C [3]. The amount of scale that is formed depends upon the forging temperature to which the steel is heated and the length of heating time.

The scale is a waste of material and must be cleaned before billet is forged between the forging die. A scale allowance has to be applied to the calculations of the billet volume. Bruchanow and Rebelski [3] recommended the values given in Table.1.2 for the calculation of scale allowance. The induction heating forms minimum scale on the surface of the heated billet and minimum scale allowance is added to the value of required billet volume.

Table 1.2 Scale Allowance Values [3]

Type of Furnace	Scale Allowance
Oil Box Furnace	4 %
Gas Box Furnace	3 %
Gas Continuous Heating Furnace	2.5 %
Electric Resistance Furnace	1.5 %
Induction Heating Furnace	1 %

1.3 Basics of Induction Heating

Induction heating is simply a method that uses electrical magnetic field to heat the conducting materials by the help of materials electrical resistivity property. The source of the electrical magnetic field is the electrical current flowing inside the coil that is suitable dimensioned and placed according to work piece geometry. Against this magnetic field, eddy currents are formed by the conducting material inside itself. These eddy currents and the electrical resistance of the material create heat inside the material according to the Joule's law [4]. The most interesting side of the method is that heating occurs without contact and by this way locally and precise heating can be applied. The amount of heat created by induction heating is depend on the several independent parameters such as power supplied, induction heating time, workpiece geometry, material properties, workpiece positioning in the coil, coil structure geometry, number of turning in the coil and also induction power supply frequency . Figure 1.1 represents the schematic view of the induction heating mechanism.
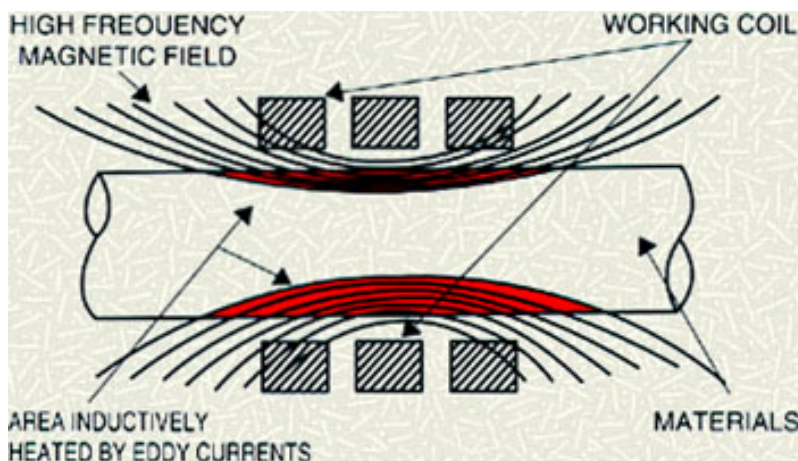
Figure 1.1 Schematic View of Induction Heating Mechanism

Induction heating mechanism is highly related with the magnetic field theory and transformation of the electrical energy to the heating energy. The English physicist Michael Faraday (1831) first discovered the magnetic field and electro-motive force (emf). His law states that a magnetic field changing in time creates a proportional electro-motive force [4]. Which means for the inducting heating that an alternating current applied to the induction coil will result wilt the magnetic field formed around coil. The German physicist Lenz (1833) states that inductive current flows inverse to the direction of changes in induction magnetive movement. Also another physicist Leon Foucault in 1851, discovered the eddy current (also known as Foucault current) caused by a moving magnetic filed intersecting with a conductor, the relative motion causes a circulating flow of electrons, or current, within the conductor [4]. These circulating eddies of current create electromagnets with magnetic fields that oppose the change in the external magnetic field. Figure 1.2 indicates the opposing direction of the coil current and the induced eddy current. The stronger the magnetic field, or greater the electrical conductivity of the conductor, the greater the currents developed and the greater the opposing force. In other words, opposing the coils magnetic field workpiece form its own magnetic field by introducing eddy current inside itself. These eddy currents transform the electrical energy to heating energy by the electrical resistance of the material according to Joule's law. Joule's heating law (1840) states that the conductor temperature increases as a result of electrical current flowing through it [4].

$$Q = I^2 \cdot R \cdot t \qquad (1.1)$$

Where Q is the heat generated by a constant current I, flowing through a conductor of electrical resistance R, for a time t.
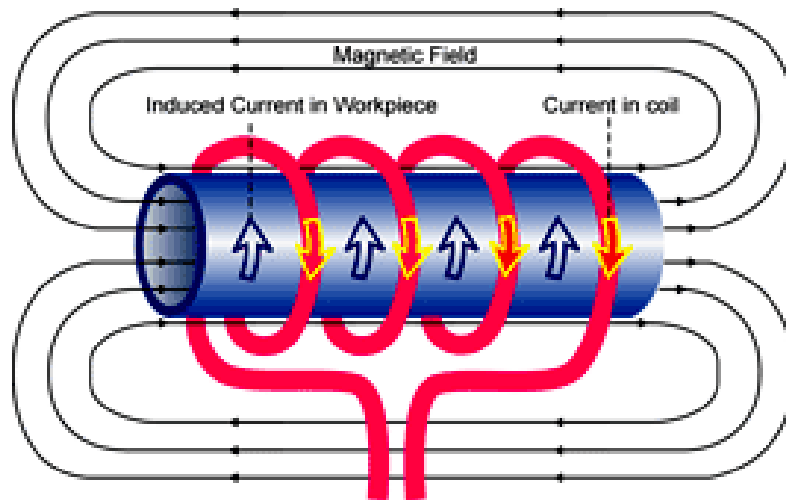
Figure 1.2 Induced Eddy Current and the Coil Current Directions

Material properties of the heated workpiece determine the heating pattern and the amount of heat created. Magnetic materials are easier to heat than non-magnetic. In magnetic materials, induction heating has two modes of heat generation: one and the main source of the heat is the resistive heat generation that is same with the non-magnetic materials and the other one is hysteresis effect of heating [7]. Hysteresis effect results from magnetic materials response to the rapidly changing magnetic field. These materials naturally resist the rapidly changing magnetic fields within the induction coil therefore resulting friction produces its own additional heat hysteresis heating in addition to eddy current heating. The contribution of hysteresis heating does not exceed 7 % of the eddy current heating in most of the application like heating of billet in hot forging [1]. Then, it is neglected during the calculation of required heating power.

Induction heating is dependent on the several parameters that some parameters are related with material properties and the others are related with the operation conditions. The main material properties are the electrical resistivity and the relative magnetic permeability of the metal. Electrical resistivity is the property of material that measured how easily conducts electrical current [7]. The electrical resistivity is temperature dependent property and increases with the increasing temperature. Magnetic permeability is the measure of the material magnetization to the response of applied magnetic flux [1]. The measurement based on the comparison with the vacuum is called relative magnetic permeability. The magnetic flux density and the temperature are the main factors affecting the relative magnetic permeability. Materials are divided into three groups according to their magnetization ability: ferromagnetic, diamagnetic and paramagnetic [7]. Ferromagnetic materials have greater permeability values than the vacuum and gives better response to the induced magnetic field but the ferromagnetic material become nonmagnetic material at the temperature called curie temperature.

Induction heating systems works with the alternating current, as a result the induced current inside the workpiece is concentrated at the outer surface with a thickness called penetration thickness (depth). This effect is also named as skin effect. The heat generation take place in this penetration part therefore material heated from surface (skin) to core. The depth of penetration is proportional to both the material properties electrical resistivity, relative magnetic permeability and the process factor frequency. Changing the frequency the penetration depth as a result the heat generation depth will change for a specific material. The high frequencies (i.e.10 000 Hz – 1000 Hz) are used for thin materials and the low frequencies (i.e. 1000 Hz -50 Hz) are preferred for the relatively thick materials.

1.4 Induction Heating Furnaces and Units

Induction heating furnaces basically consist of two main units and some supporting units that are changing with the machine capacity. One of the main units is the power supply unit. Power supply unit generates required amount of current with the proper voltage and frequency to the working induction coil. Voltage and the current controls the power transferred to the workpiece. The working frequency controls the magnetic field penetration depth to the workpiece which means the heat generation depth inside the workpiece. However, the working frequency is fixed and does not change for a certain induction heater. Therefore, there is a limitation on the cross-section of the workpiece that the induction heater can generate heat inside the material.

Another main unit of the induction heating system is the induction coil box. The induction coil box is composed of copper made helical coil and the refractor cover around the copper coil. The coil generated the magnetic field around the workpiece. Figure 1.3 shows the induction heater and some main units of the induction heater.
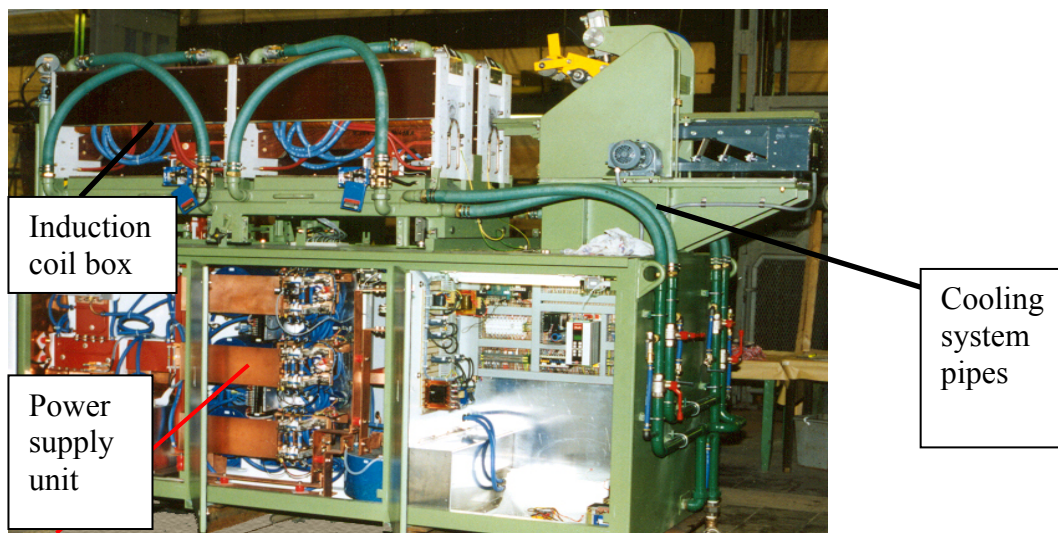
Figure 1.3 Units of Induction Heating Furnace

The subunits of the induction heating system will change according to the heating purpose and the capacity of the system but generally the cooling system is one of the subunit that should be placed into the system to cool down working coil and the power unit. For this purpose, the coil made up with copper tubes. Inside these tubes, distillated water that is not conducting electrical current is circulating to remove heat from the coil. Additionally, workpiece loading subunit will be needed for feeding the workpiece to the coil and sequentially heat them. The heated parts move on rail and each part pushes the other one. Then, when the new workpiece enters the coil, the heated part will leave with in the same time.

Another subunit will be the temperature measurement unit. Generally optic pyrometer measures the temperature of the workpiece. The optic pyrometer placed at the end of the coil will measure the temperature of the heated workpiece. Figure 1.4 demonstrates these sub-units of the induction heater.
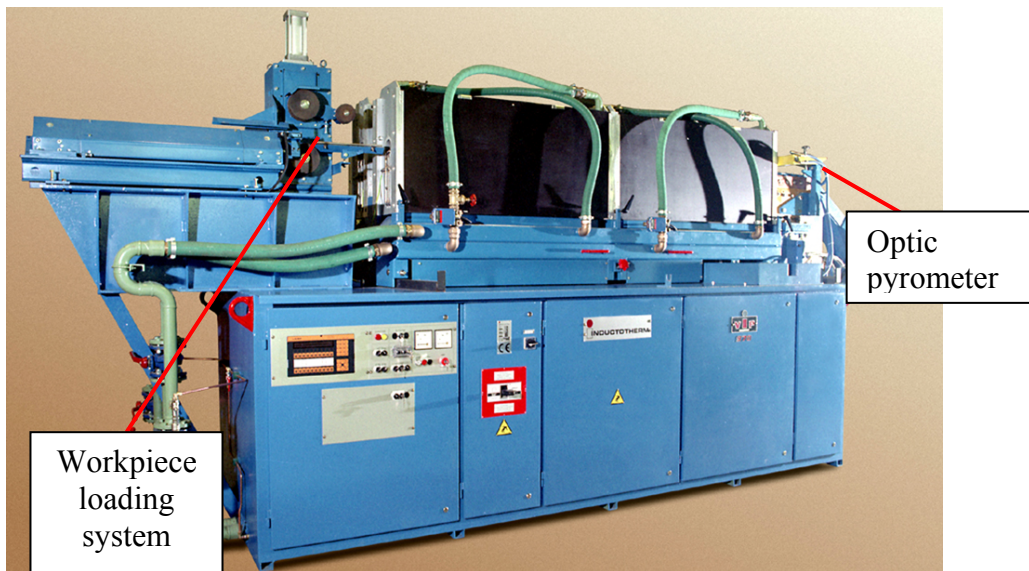
Figure 1.4 Sub-units of the Induction Heating Furnace

1.5 Some Previous Studies Related with the Induction Heating

Some previous studies have been conducted on induction heating method. The electrical control unit and the dynamic of the controlling unit of the induction heater are investigated by J. Nerg and K. Tolsa [13]. H. Shen et al [14] studied on temperature field induced in high frequency induction heating. J. Y. Jang and Y. W. Chiu [15] worked on the numerical and experimental thermal analysis for a metallic hollow cylinder subjected to stepwise electro-magnetic induction heating. V. Rudnev [16] has studied on induction heating and induction coil failures. S. C. Chen et al [17] have worked on the simulations and verification of induction heating on a mold plate. O. Okman [18] has studied on locally heating of billets.

1.6 Scope of the Thesis

The industrial applications of the induction heating, hot forging application and advantages of the induction heating in hot forging have been described in previous sections. The induction heating furnace units and the operating parameters have also been mentioned basically. It is stated that the resultant temperature of the heated billet is strongly effected with operating parameters of the induction heating furnace such as power supplied, conveyor speed and the induction coil box hole diameter.

The aim of this study is investigating the relations between resultant temperature of the heated billet and the operating parameters of the induction heater which are, heating power supplied, conveyor speed and induction coil box hole diameter.

The relations will be investigated by using the results of the real life experiments. The experiments will be planed according to Design of Experiment Method. The main and the interaction effects of these parameters on the temperature of the heated billet will be investigated. The linear regression model will be applied for the derivation of the temperature prediction formula.

The experiments will be performed by using the 125 KW 3000 Hz induction heater together with different coil boxes that are available in METU-BILTIR CENTER. The temperatures of the heated billets will be measured by using optical pyrometer.

The details of the induction heating theory, the effects of material properties and the operating conditions on the induction heating will be described in Chapter 2.

The Design of Experiment Method, analysis of the main and the interaction effects of factors on the objective output will be explained in Chapter 3. The linear regression model and the derivation of the prediction formula will also be demonstrated in Chapter 3.

The experimental set-up of induction heater and induction coils, test specimen selection, temperature measuring optic pyrometer and experimental procedure will be described in Chapter 4.

In Chapter 5, the results of the different values of factors will be examined for the main and the interaction effects on the heated billet temperatures. A formula will be derived by using multiple linear regression technique, to be used to predict the resultant temperature of the heated billet.

Finally, general conclusions of the experiments and suggestions for future works will be given in Chapter 6.

CHAPTER 2

THEORY OF INDUCTON HEATING

The analysis of induction heating is complex operation since the induction heating is combination of electro-magnetic process with the heat transfer phenomena. The relation between them are highly interrelated because, the source of the heat is electro-magnetic originated and both the thermal and the electro magnetic properties of the materials are highly temperature dependent and changing non linear with the increasing temperature. Then the problem becomes complicated.

The heat generation source is mainly due to the electrical resistance of the material according to Joule law [4]. The power that is transferred to the workpiece changes with voltage and current applied to system and the electrical resistance of the subjected material. Both the induced current amount and the electrical resistance are related with the material properties. The main material properties that are considered to analyze come out the electrical resistance and the electro magnetic properties of the materials.

2.1 Electrical Resistance

Electrical resistance (R) is material property both related with the geometry and electrical resistivity characteristic of the material. Electrical resistance is directly proportional to the electrical resistivity ρ and length of the material l; however it is inversely proportional to the cross-section of the current flowing direction A_c [9].

$$R = \frac{\rho \cdot l}{A_c} \qquad (2.1)$$

Electrical resistivity ρ indicates the material ability to conduct electrical current. Generally electrical resistivity of metals increases with the increasing temperature. The resistivity of the pure metals can often be represented as linear function of the temperature. Table 2.1 shows the values of electrical resistivity and temperature coefficients for some commonly used materials at room temperatures.

Table 2.1 Electrical resistivity and temperature coefficients of some commonly used materials [1]

Materials at Room Temperature	Electrical Resistivity $(\Omega \cdot m)$	Temperature coefficient $(1 / {}^{\circ}C)$
Silver	1.59×10^{-8}	0.0061
Copper	1.68×10^{-8}	0.0068
Gold	2.44×10^{-8}	0.0034
Aluminum	2.65×10^{-8}	0.0043
Tungsten	5.60×10^{-8}	0.0045
Zinc	5.91×10^{-8}	0.0042
Nickel	6.80×10^{-8}	0.0069
Cobalt	9.00×10^{-8}	0.0053
Mild Carbon Steel	15.9×10^{-8}	0.0061
Stainless Steel	70.0×10^{-8}	0.0061
Lead	1.59×10^{-8}	0.0061

The resistivity of the pure metals can generally be represented as a linear function of the temperature [1]:

$$\rho(T) = \rho_0 \, (1 + \alpha(T - T_0)) \qquad\qquad (2.\,2)$$

Where the ρ_0 is the resistivity at ambient temperature T_0, $\rho(T)$ is the resistivity at temperature T, and the α is the temperature coefficient of the electrical resistivity. The resistivity of a small number of materials decreases with the temperature and α values can be negative. For the other materials α is a nonlinear function of the temperature [1].

The electrical resistivity values of some materials for different temperatures are represented in Figure 2.1. It is seen that all the material represented in the graph have increase in electrical resistivity values with increasing temperature. This indicates that during the induction heating, as the temperature of the workpiece increases the electrical resistance of the material also increases and results with the amplified heating effect.
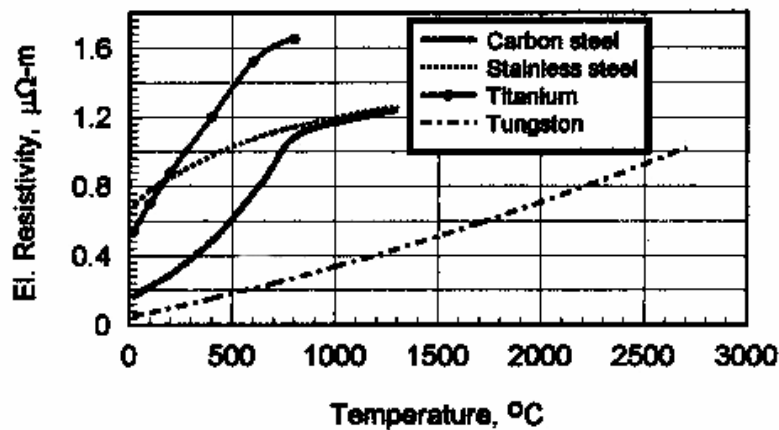
Figure 2.1 Electrical Resistivity versus Temperature [1]

2.2 Relative Magnetic Permeability

The magnetic permeability is the relative decrease or increase in the magnetic field inside the material compared with the magnetic field in which the material is located [1]. Magnetic permeability μ is defined as

$$\mu = \frac{\mathbf{B}}{\mathbf{H}}$$ (2. 3)

where μ is magnetic permeability in Henry per m (H/m), $\mathbf{B}$ is magnetic flux density in Tesla (T) and $\mathbf{H}$ is magnetic field strength in Amperes per meter (A/m).

Relative magnetic permeability μ_r is the comparsion value, it is the ratio of magnetic permeability value of the material to free space permeability as follows

$$\mu_r = \frac{\mu}{\mu_o}$$ (2. 4)

where μ_0 is permeability of vacuum and the value of μ_0 is $4\pi \times 10^7$ H/m [1].

Materials are divided into three groups according to their magnetization ability: ferromagnetic, diamagnetic and paramagnetic. Ferromagnetic materials have greater permeability values than the vacuum (i.e. $\mu_r \gg 1$) and show large and positive susceptibility to the external magnetic field. Diamagnetic material have slightly greater relative permeability than 1 (i.e. $\mu_r > 1$) and paramagnetic materials have slightly less relative permeability value than 1 (i.e. $\mu_r < 1$). Both paramagnetic and the diamagnetic materials can be called nonmagnetic materials. Magnetic permeability value changes with the changing magnetic filed intensity and the temperature.
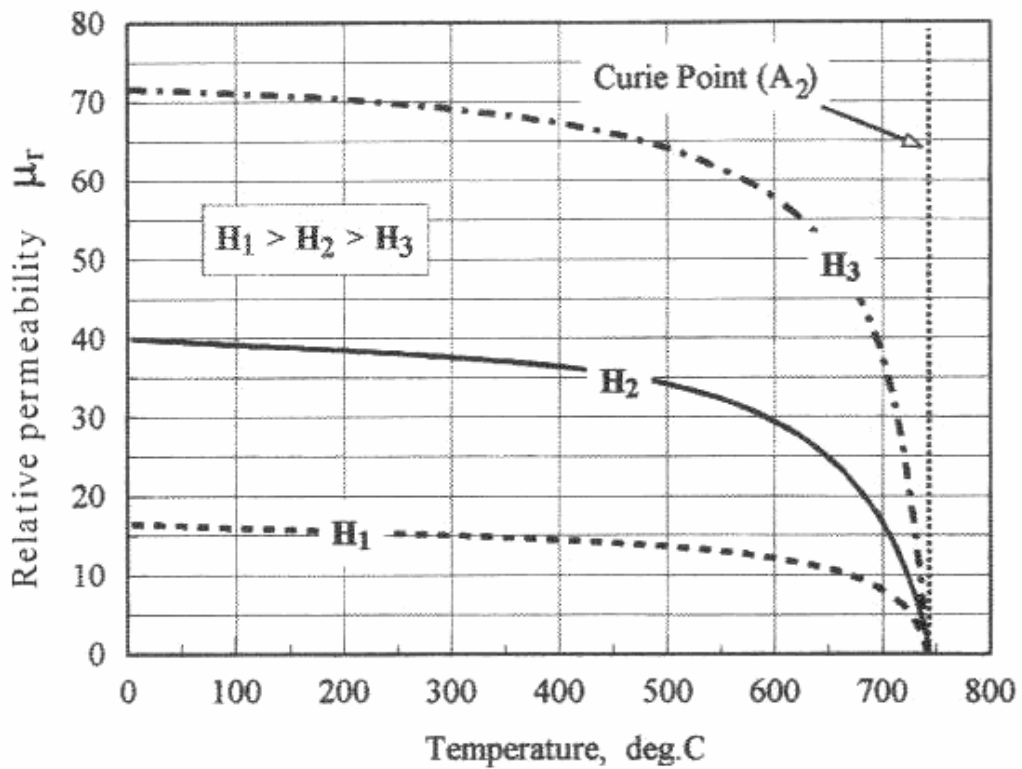
Figure 2.2 Effect of temperature and magnetic field intensity on relative
permeability of medium carbon steel [1]

The variations of the relative magnetic permeability with respect to temperature and the magnetic field intensity are represented in Figure 2.2. The magnetic permeability of the specimen in three different values of magnetic field strength, H_1, H_2 and H_3 is presented. As the field strength increases the relative magnetic permeability values decreases. In a similar way when the temperature reaches around the 500 ^oC, the relative magnetic permeability values sharply drops and at the temperature called Cure Point ($\sim$740 ^oC) becomes zero. Figure 2.3 shows the three dimensional distribution of the magnetic permeability with respect to temperature and the magnetic flux density.
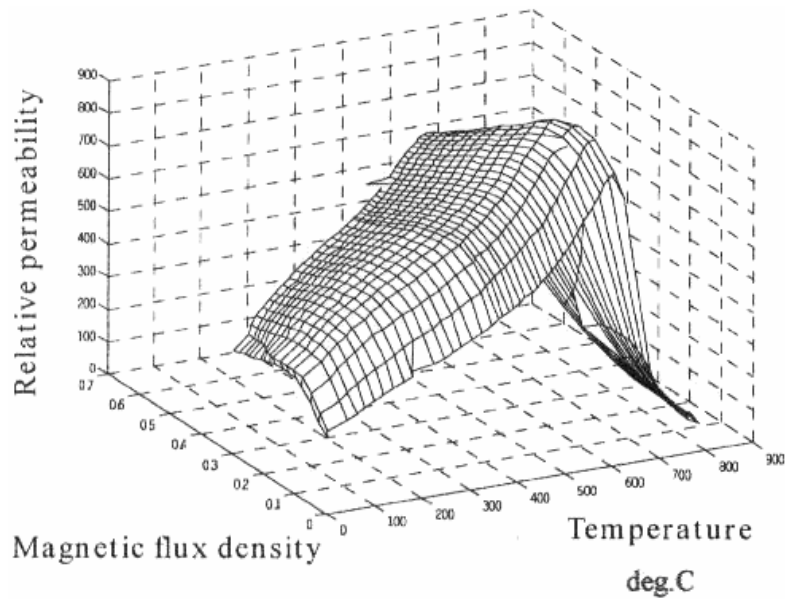
Figure 2.3 Three dimensional distribution of the relative permeability [7]

Ferromagnetic materials become nonmagnetic at the temperature called Curie temperature. At Curie temperature, the magnetic materials start to behave as if they are non-magnetic. Curie point of magnetic materials changes with the chemical composition of the material. For example plain carbon steel AISI 1008 has the curie temp 768 $^{\circ}$C and the other plain carbon steel AISI 1060 has the 732 $^{\circ}$C. The difference originated from carbon content of the material [1].
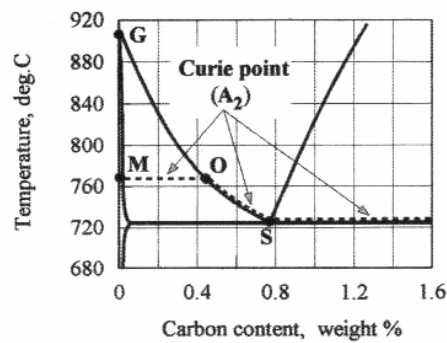
Figure 2.4 Curie temperature of the plain carbon steel [1]

Magnetic field intensity H, decreases exponentially from maximum point at surface to minimum value at the core during the induction heating. On the other hand, the relative permeability also varies within the workpiece. Starting from surface value, relative permeability increases and at a certain point it takes maximum value then it begins decreasing as moving to the core. Figure 2.5 represents the distribution of the magnetic field intensity and the relative magnetic permeability along the homogenous carbon steel cylinder
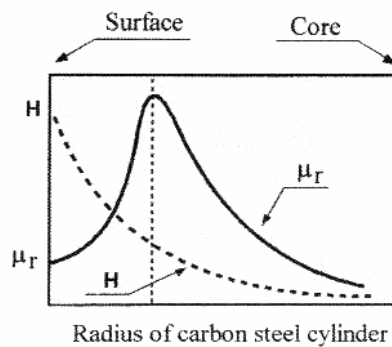
Figure 2.5 Distribution of the magnetic field intensity H and the relative magnetic permeability μ_r along the homogenous carbon steel cylinder [1]

2.3 Frequency and Penetration Depth

Frequency and the penetration depth are the significant factors in induction heating. In high frequency induction heating, induced alternating current is not uniform throughout the workpiece cross-section. It is concentrated at the surface. This effect is called skin effect [9]. The current distribution in the conducting material will decrease exponentially from surface to core. Figure 2.6 represents current distributions in induction coil and the workpiece. Approximately the 86 % percentage of the power will be concentrated on the surface of the conductor. The thickness of this layer is called skin depth or penetration depth.

The degree of penetration depth is depend on the frequency of the current and both the material properties electrical resistivity and the magnetic permeability of the conductor.

The current density along the work piece thickness (radius) can be calculated by the following equation [9]:

$$I = I_0 e^{-y/\delta} \tag{2.5}$$

Where the I is the current density at distance y from the surface (A/m^2); I_0 is the current density at the workpiece surface (A/m^2), y is the distance from surface toward the core (m) and δ is penetration depth (m).
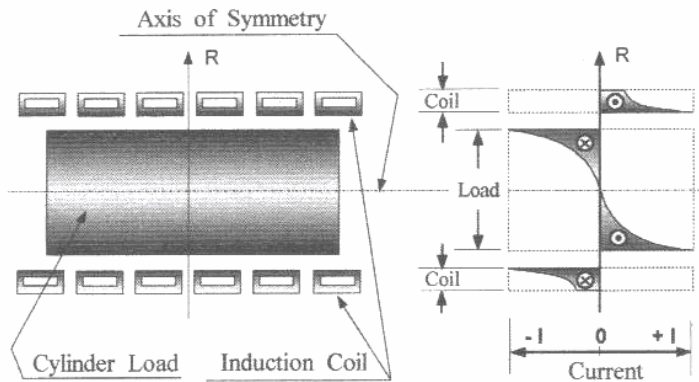
Figure 2.6 Current distributions in induction coil and the workpiece [1]

Penetration depth is described in meter as [9];

$$\delta = 503 \cdot \sqrt{\frac{\rho}{\mu_r F}} \tag{2.6}$$

Where ρ : electrical resistivity of the conductor $\Omega \cdot m$,
 μ_r : Relative magnetic permeability
 F : Frequency, Hz

The penetration depth is not only related with the material properties like electrical resistivity and the relative magnetic permeability but also process parameter frequency. Since the material properties changes with the temperature, during the heating, the penetration depth varies significantly. Figure 2.7 indicates the change in skin depth against the temperature increase. At the beginning of the heating cycle, the current penetration into the carbon steel work piece will increase slightly because of the increase in the electrical resistivity. After a further rise in temperature (near 550 $^{\circ}$C) the relative permeability suddenly drops as a result the penetration depth will increase rapidly. At the Curie temperature relative permeability becomes unity and the increase in the penetration depth slow downs and start to increase with the changing electrical resistivity resulted from temperature increase.
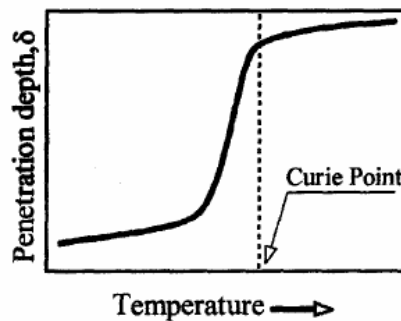
Figure 2.7 Variation of skin depth during induction heating of a carbon steel workpiece [1]

In addition to skin effect, electro magnetic proximity effect can be mentioned for the thin materials. In thin materials it is possible that the magnetic fields overlap each other or unevenly distributed and may cancel each other or it may strength the magnetic field. This effect is named as electromagnetic proximity effect.

2.4 Mathematical Modeling of the Electromagnetic Field

The time varying electro-magnetic field transports the energy to the workpiece by means of electro-magnetic waves. The change in electric field generates magnetic field or in the contrary the change in the magnetic field results with electric field. For a linear and isotropic media, the following relation is valid between the electric field (**E**) and the electric field (**D**), where ε is the absolute permittivity of the medium and measured in farads per meter (F/m) [1].

$$\mathbf{D} = \varepsilon\mathbf{E} \tag{2.7}$$

The relationship between the magnetic flux density and the magnetic field intensity is described by the formula, where μ is the absolute magnetic permeability of the material.

$$\mathbf{B} = \mu\mathbf{H} \tag{2.8}$$

Within a conducting material, the conduction of currents is a result of the drift motion of charge carriers due to the presence of an electric field. This phenomenon is formulized by the *Ohm's Law,* given below.

$$\mathbf{J} = \frac{1}{\rho}\mathbf{E} \tag{2.9}$$

In this formula, **J** represents the volume current density, **E** is the electric field and ρ is the electrical resistivity of the material. Under time varying conditions, an electromagnetic model should be constructed, which relates the magnetic field vectors **B** and **H** to the electric field vectors **E** and **D**. The set of equations used to describe the electromagnetic field are called the *Maxwell's Equations* [1].

$$\nabla \times \mathbf{E} = -\frac{\partial \mathbf{B}}{\partial t} \tag{2.10}$$

$$\nabla \times \mathbf{H} = \mathbf{J} + \frac{\partial \mathbf{D}}{\partial t} \tag{2.11}$$

$$\nabla \cdot \mathbf{D} = \rho_v \qquad\qquad (2.12)$$

$$\nabla \cdot \mathbf{B} = 0 \qquad\qquad (2.13)$$

Equation 2.10 is known as the *Faraday's law*. It is the quantitative representation of the experimental observation that magnetic flux change in a medium will result in induction of current in a conducting loop that is linked to it. The physical interpretation of equation 2.11 is that whenever there is a time varying electric field in a medium, a magnetic field will induced, even in the absence of free current flow. The equation 2.12 is the divergence relation between the electric field and the distribution of free charges in a medium. It is a fundamental governing equation for electrostatics in any medium. The symbol ρ_v denotes the volume density of free charges [1].

Substituting equation 2.8 into equations 2.10 and 2.13 the following form can be achieved.

$$\nabla \times \mathbf{E} = -\frac{\partial(\mu\mathbf{H})}{\partial t} \qquad\qquad (2.14)$$

$$\nabla \cdot (\mu\mathbf{H}) = 0 \qquad\qquad (2.15)$$

In a similar way substituting equation 2.7 and 2.9 into equation 2.11 and 2.12 the following form can be achieved.

$$\nabla \times \mathbf{H} = \frac{\mathbf{B}}{\rho} + \frac{\partial(\varepsilon\mathbf{E})}{\partial t} \qquad\qquad (2.16)$$

$$\nabla \cdot (\varepsilon\mathbf{E}) = \rho_v \qquad\qquad (2.17)$$

22

The magnetic flux density $\mathbf{B}$, can be expressed in terms of a magnetic vector potential $\mathbf{A}$ as follows $\mathbf{B} = \nabla \times \mathbf{A}$. By introducing the electrical scalar potential ϕ, which satisfies $\nabla \times \nabla \phi = 0$. Then

$$\mathbf{E} = -\frac{\partial \mathbf{A}}{\partial t} - \nabla \phi \qquad (2.18)$$

Substituting $\mathbf{B} = \nabla \times \mathbf{A}$ into equation 2.16, one can obtain

$$\frac{1}{\mu} \nabla^2 \mathbf{A} = -\frac{\partial \varepsilon \mathbf{E}}{\partial t} - \frac{\mathbf{E}}{\rho} \qquad (2.19)$$

After substituting equation 2.18 into equation 2.19, the electro-magnetic field equation in terms of $\mathbf{A}$ and ϕ is given below

$$\frac{1}{\mu} \nabla^2 \mathbf{A} = \varepsilon \frac{\partial^2 \mathbf{A}}{\partial t^2} + \varepsilon \frac{\partial \nabla \phi}{\partial t} + \frac{1}{\rho} \frac{\partial \mathbf{A}}{\partial t} + \frac{1}{\rho} \nabla \phi \qquad (2.20)$$

Where the $\varepsilon \dfrac{\partial^2 \mathbf{A}}{\partial t^2} + \varepsilon \dfrac{\partial \nabla \phi}{\partial t}$ is the displacement current density, $\dfrac{1}{\rho} \dfrac{\partial \mathbf{A}}{\partial t}$ is the eddy current density, $\dfrac{1}{\rho} \nabla \phi$ or $(-\mathbf{J})$ is the conduction current density. For the most practical applications, the displacement current can be neglected, thus the equation 2.20 can be simplified as:

$$\frac{1}{\mu} \nabla^2 \mathbf{A} + \mathbf{J} - \frac{1}{\rho} \frac{\partial \mathbf{A}}{\partial t} = 0 \qquad (2.21)$$

When the electro-magnetic field quantities are harmonically oscillating functions with the a single frequency F, and the **A** can be expressed as

$$\mathbf{A}(x,y,z,t) = A(x,y,z)e^{j\omega t}$$ where $j = \sqrt{-1}$, A and the $\omega = 2\pi F$ is the angle frequency. Substituting these into above equation one can obtain following equation,

$$\frac{1}{\mu}\nabla^2\mathbf{A} + \mathbf{J} - \frac{1}{\rho}j\omega A = 0 \tag{2.22}$$

The time dependent heat transfer process in a steel cylinder can be described by Fourier equation.

$$k(\nabla^2 T) + \dot{q} = dc_p \frac{\partial T}{\partial t} \tag{2.23}$$

Where the T is temperature, k is thermal conductivity, d is density, c_p is the heat capacity and $\dot{q}$ is the heat source density induced by eddy current per unit time in a unit volume. The heat source density is related to conduction current density by Joule heating law as shown below.

$$\dot{q} = \mathbf{J}^2 \rho = \frac{1}{\rho}(\frac{\partial \mathbf{A}}{\partial t})^2 = \frac{1}{\rho}(\frac{\partial (Ae^{j\omega t})}{\partial t})^2 = \frac{1}{\rho}(j\omega Ae^{j\omega t})^2 \tag{2.24}$$

CHAPTER 3

DESIGN OF EXPERIMENT

Experimental analysis can be planed and conducted by using Design of Experiment Method. To provide a basis for the current study, Design of Experiment Method and 2^3 Factorial Design which are described by Montgomery D.C. [10] will be reviewed in the following sections.

3.1 Design of Experiment Method

Design of Experiment Method is organized method that is used to determine the relationship between the different factors affecting a process and the output of that process. Instead of one factor at a time approach, experimental strategies are used in practice to reduce the number of experiments. In this method, first it is selected the factors affecting the objective output of the process. The range, highest and the lowest values, that is going to be used in the experiments for each factor have to be determined. Then, experiments are performed by applying each factor in these limiting values while keeping the other factors constant. The most important part of this method is that, this method considers the interactions effects between the factors and their effect on the process when they are changed together. However, one factor at a time strategy fails to consider any possible interaction between the factors. Therefore, the factorial experiment method is used to find out the interaction effects of the factors.

3.2 The 2^3 Factorial Design of Experiment Method

The 2^k factorial design approach is simple and small numbers of experiments are needed to achieve good results including the interaction effects [19]. The number of the controlled parameters is 3 so the design is called a 2^3 factorial design and eight different experiments will be used.

When there is need to examine the effects of three factors on a process than the 2^3 Factorial Design of Experiment Method can be used. The effect of these parameters on a process will be examined in experimental study by fixing other parameters. 2^3 Factorial Design Method will be used to include the interaction effects of the parameters on a process. The geometric view of the 2^3 factorial design for the treatment combinations can be shown as a cube as illustrated in Figure 3.1. The three factors are named as A, B and C. Lowercase letters denotes the factors that are at high level at that application.
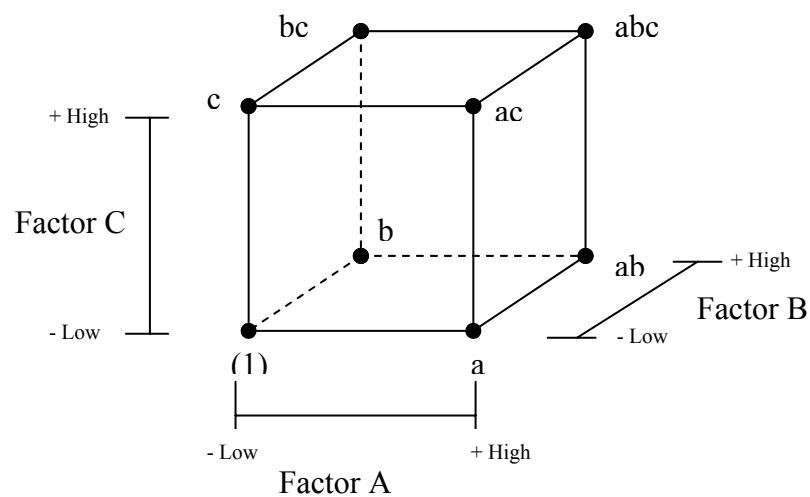
Figure 3.1 Geometric View of the 2^3 Factorial Design [11]

The main effect of A can be calculated by considering the effect of A in different conditions. When the effect of A is high and other two factors B and C are at low level, the effect of A is [a-(1)]/n, where n is the number of different measurements. Similarly, when A and B are at high level and C is at the low level, the effect of A is [ab-b]/n and when A and C are at the high level and B is at the low level, the effect of A is [ac-c]/n. Finally, when all the factors A,B,C are at high levels, the effect of A is [abc-bc]/n [19].

The summation of all these effects gives the average main effect of A

$$A = \frac{1}{4n}\left[a - (1) + ab - b + ac - c + abc - bc \right] \qquad (3.1)$$

Similar derivations are done to for investigation of the average main effect of both B and C. The following equations are achieved:

$$B = \frac{1}{4n}\left[b - (1) + ab - a + bc - c + abc - ac \right] \qquad (3.2)$$

$$C = \frac{1}{4n}\left[c - (1) + ac - a + bc - b + abc - ab \right] \qquad (3.3)$$

The one-half difference between the averages A effects at the two levels of B gives the AB interaction formula. At high level of B the A effects are [abc-bc]/n and [ab-b]/n. So the average A effect for the high levels of B is;

$$\frac{\left[(abc - bc) + (ab - b) \right]}{2n} \quad \text{(average A effect at high level B)} \qquad (3.4)$$

In a similar way the A effect at low level B is;

$$\frac{[(ac - c) + (a - (1)]}{2n} \text{ (average A effect at low level B)} \qquad (3.5)$$

The difference of average A effects is;

$$\frac{[abc - bc + ab - b - ac + c - a + (1)]}{2n} \qquad (3.6)$$

As AB interaction is found by taking the one-half difference of average A effects which is;

$$AB = \frac{[abc - bc + ab - b - ac + c - a + (1)]}{4n} \qquad (3.7)$$

Similar derivations are done for the investigation of average main effects of AC and BC.

$$AC = \frac{[(abc - bc + ac - c - ab + b - a + (1)]}{4n} \qquad (3.8)$$

$$BC = \frac{[(abc - ac + bc - c - ab + a - b + (1)]}{4n} \qquad (3.9)$$

The ABC interaction is defined as the average differences between the AB interactions for the two different levels of C. The calculated ABC interaction is

$$ABC = \frac{1}{4n}[(abc - bc) - (ac - c) - (ab - b) + (a - (1))]$$

$$(3.10)$$

$$ABC = \frac{[abc - bc - ac + c - ab + b + a - (1)]}{4n}$$

The quantities in the brackets in numerators are called contrasts in the treatment combinations. Using these contrasts the Table 3.1 is developed with plus and minus signs [11].

Table 3.1 Algebraic Signs for Calculation of Effects in the 2^3 Design [11]

Factorial Effect	Treatment Combination							
	1	a	b	ab	c	ac	bc	abc
A	-	+	-	+	-	+	-	+
B	-	-	+	+	-	-	+	+
C	-	-	-	-	+	+	+	+
AB	+	-	-	+	+	-	-	+
AC	+	-	+	-	-	+	-	+
BC	+	+	-	-	-	-	+	+
ABC	-	+	+	-	+	-	-	+

3.3 Derivation of Formula

Using the results of the experiments, a formula can be derived to predict the possible outputs of the process. Formula can be derived by using Linear Regression Technique. The results of the experiments will be fitted to response surface. In the following sections the derivation of a formula for 2^3 Factorial experiment results will be explained.

3.3.1   Linear Regression Models

A first-order response surface model that might describe a relationship as follows

$$y = \beta_0 + \beta_1 x_1 + \beta_2 x_2 + \varepsilon \qquad (3.11)$$

This is a multiple linear regression model with two independent variables x_1 and x_2. The dependent variable y represents the response and ε represents the error. Equation is a linear function of the unknown parameters β_0, β_1 and β_2. The model describes a plane in the two dimensional x_1, x_2 space.

29

The parameter β_0 defines the intercept of the plane [19]. The parameters, β_1 and β_2 are called the partial variable coefficients, because β_1 measures the expected change in y per unit change in x_1 when x_2 is held constant, and β_2 measures the expected change in y per unit change in x_2 when x_1 is held constant [19].

The response may be related to k independent variables and the model is

$$y = \beta_0 + \beta_1 x_1 + \beta_2 x_2 + \dots\dots\dots + \beta_k x_k + \varepsilon \tag{3.12}$$

This is called a multiple linear regression model with k variables. The parameter β_i represents the expected change in response y per unit change in x_i when all the independent variables are held constant [19].

When interaction terms are added to the first order model the new equation become more complex with respect to Equation 3.20.

$$y = \beta_0 + \beta_1 x_1 + \beta_2 x_2 + \beta_{12} x_1 x_2 + \varepsilon \tag{3.13}$$

Where $x_1 x_2$ is an interaction term and β_{12} is the variable coefficient of it. If they are defined like $x_3 = x_1 x_2$ and $\beta_3 = \beta_{12}$. The equation becomes

$$y = \beta_0 + \beta_1 x_1 + \beta_2 x_2 + \beta_3 x_3 + \varepsilon \tag{3.14}$$

This is also a standard multiple linear regression model with three independent variables.

3.3.2 Linear Regression Models for 2^3 Factorial Design

In order to form a model for a 2^3 Factorial Design, all the main terms and interaction terms have to be included in the equation. The main effects terms can be classified as x_1, x_2, x_3 and the interaction effects terms are $x_1 x_2$, $x_1 x_3$, $x_2 x_3$ and $x_1 x_2 x_3$. The variable coefficients of these terms are β_1, β_2, β_3, β_{12}, β_{13}, β_{23} and β_{123}. As a result the model is written as;

$$\begin{aligned} y = \beta_0 + \beta_1 x_1 + \beta_2 x_2 + \beta_3 x_3 + \beta_{12} x_1 x_2 \\ + \beta_{13} x_1 x_3 + \beta_{23} x_2 x_3 + \beta_{123} x_1 x_2 x_3 + \varepsilon \end{aligned} \tag{3.15}$$

By substituting the interaction effects as, $x_1x_2 = x_4$, $x_1x_3 = x_5$, $x_2x_3 = x_6$, $x_1x_2x_3 = x_7$ and substituting their variable coefficients such as $\beta_{12} = \beta_4$, $\beta_{13} = \beta_5$, $\beta_{23} = \beta_6$ and $\beta_{123} = \beta_7$ then equation becomes [19],

$$y = \beta_0 + \beta_1 x_1 + \beta_2 x_2 + \beta_3 x_3 + \beta_4 x_4 + \beta_5 x_5 + \beta_6 x_6 + \beta_7 x_7 + \varepsilon \qquad (3.16)$$

3.3.3 Estimation of the Parameters in Linear Regression Models

The method of least squares is typically used to estimate the regression coefficients in a multiple linear regression model. Suppose that n>k observations on the response variable are available. The model equation in terms of the observations is,

$$y_i = \beta_0 + \beta_1 x_{i1} + \beta_2 x_{i2} + \ldots\ldots\ldots + \beta_k x_{ik} + \varepsilon_i$$

$$y_i = \beta_0 + \sum_{j=1}^{k} \beta_j x_{ij} + \varepsilon_i \qquad i = 1,2,3\ldots,n \qquad (3.17)$$

The sum of the squares of error is taken, so the error is minimized. The least squares function is [11],

$$L = \sum_{i=1}^{n} \varepsilon_i^{\,2}$$

$$L = \sum_{j=1}^{n} (y_i - \beta_0 - \sum_{j=1}^{k} \beta_j x_{ij})^2 \qquad (3.18)$$

The function L is to be minimized with respect to β_0, β_1..., β_k. The least squares estimators, say $\hat{\beta}_0, \hat{\beta}_1, \ldots\ldots\ldots \hat{\beta}_k$, must satisfy

$$\left. \frac{\partial L}{\partial \beta_0} \right|_{\hat{\beta}_0, \hat{\beta}_1 \ldots, \hat{\beta}_k} = -2 \sum_{j=1}^{n} (y_i - \hat{\beta}_0 - \sum_{j=1}^{k} \hat{\beta}_j \, x_{ij}) = 0 \qquad (3.19a)$$

and

$$\left. \frac{\partial L}{\partial \beta_j} \right|_{\hat{\beta}_0, \hat{\beta}_1 \ldots, \hat{\beta}_k} = -2 \sum_{j=1}^{n} (y_i - \hat{\beta}_0 - \sum_{j=1}^{k} \hat{\beta}_j \, x_{ij}) x_{ij} = 0 \quad j=1,2,\ldots, k \quad (3.19b)$$

31

Simplifying Equation 3.19,

$$n\hat{\beta}_0 + \hat{\beta}_1 \sum_{i=1}^{n} x_{i1} + \hat{\beta}_2 \sum_{i=1}^{n} x_{i2} + \ldots\ldots + \hat{\beta}_k \sum_{i=1}^{n} x_{ik} = \sum_{i=1}^{n} y_i$$

$$\hat{\beta}_0 \sum_{i=1}^{n} x_{i1} + \hat{\beta}_1 \sum_{i=1}^{n} x_{i1}^2 + \hat{\beta}_2 \sum_{i=1}^{n} x_{i1}x_{i2} + \ldots\ldots + \hat{\beta}_k \sum_{i=1}^{n} x_{i1}x_{ik} = \sum_{i=1}^{n} x_{i1}y_i$$

$$\begin{matrix} \cdot & & \cdot & & \cdot & & \cdot \\ \cdot & & \cdot & & \cdot & & \cdot \\ \cdot & & \cdot & & \cdot & & \cdot \end{matrix} \qquad (3.20)$$

$$\hat{\beta}_0 \sum_{i=1}^{n} x_{ik} + \hat{\beta}_1 \sum_{i=1}^{n} x_{ik}x_{i1} + \hat{\beta}_2 \sum_{i=1}^{n} x_{ik}x_{i2} + \ldots\ldots + \hat{\beta}_k \sum_{i=1}^{n} x_{ik}^2 = \sum_{i=1}^{n} x_{ik}y_i$$

These equations are called the least squares normal equations. It is seen that there are p=k+1 normal equations, one for each of the unknown regression coefficients. The solutions to the normal equations will be the least square estimators of the regression coefficients $\hat{\beta}_0, \hat{\beta}_1, \ldots\ldots \hat{\beta}_k$ [19].

Solving these normal equations in matrix notation is simpler. In matrix form the Equation may be written as

$$y = X\beta + \varepsilon \qquad (3.21)$$

where

$$y = \begin{bmatrix} y_1 \\ y_2 \\ \cdot \\ \cdot \\ y_n \end{bmatrix}, \qquad X = \begin{bmatrix} 1 & x_{11} & x_{12} & \ldots & x_{1k} \\ 1 & x_{21} & x_{22} & \ldots & x_{2k} \\ \cdot & \cdot & \cdot & \ldots & \cdot \\ \cdot & \cdot & \cdot & \ldots & \cdot \\ \cdot & \cdot & \cdot & \ldots & \cdot \\ 1 & x_{n1} & x_{n2} & \ldots & x_{nk} \end{bmatrix}$$

$$\beta = \begin{bmatrix} \beta_0 \\ \beta_1 \\ \cdot \\ \cdot \\ \beta_k \end{bmatrix} \quad \text{and} \quad \varepsilon = \begin{bmatrix} \varepsilon_1 \\ \varepsilon_2 \\ \varepsilon_3 \\ \varepsilon_4 \\ \varepsilon_5 \end{bmatrix}$$

In general, y is an (n x 1) matrix of the observations, X is an (n x p) matrix of the levels of the independent variables, β is (p x 1) matrix of the regression coefficients, and ε is an (n x1) matrix of the random errors [11].

In order to find the vector of least squares estimators, $\hat{\beta}$, that minimizes

$$L = \sum_{j=1}^{n} \varepsilon_1^{\,2} = \varepsilon'\varepsilon = (y - X\beta)'(y - X\beta) \tag{3.22}$$

L may be expressed as

$$\begin{aligned} L &= y'y - \beta'X'y - y'X\beta + \beta'X'X\beta \\ &= y'y - 2\beta'X'y + \beta'X'X\beta \end{aligned} \tag{3.23}$$

Because $\beta'X'y$ is a (1 x 1) matrix, or a scalar, and its transpose $(\beta'X'y)' = y'X\beta$ is the same scalar. The least squares estimators must satisfy[11]

$$\left.\frac{\partial L}{\partial \beta}\right|_{\beta} = -2X'y + 2X'X\,\hat{\beta} = 0 \tag{3.24}$$

which simplifies to

$$X'X\,\hat{\beta} = X'y \tag{3.25}$$

Equation 3.21 is the matrix form of the least squares normal equations. It is identical to Equation 3.25. The both sides of the Equation 3.25 is multiplied by the inverse of the $X'X$ so the normal equations may be solved. Therefore, the least squares estimator of β is ;

$$\hat{\beta} = (X'X)^{-1}X'y \tag{3.26}$$

33

CHAPTER 4

EXPERIMENTAL SET UP

In this part of the thesis, the experimental set up for the analysis of induction heating will be described. The experimental set up consists of induction heater accompanying with coil boxes and temperature measuring pyrometer. Selections of test specimen and preparation stages of the experiments are also introduced in this chapter.

4.1 Induction Heater

The 125KW 3000Hz induction heater that is available in the METU-BILTIR CENTER is used in heating experiments. Figure 4.1 demonstrates the induction heater. The Inductotherm trade mark induction heater works with high voltage electrical units. The induction heater can heat the billets having the diameters of Ø10 mm up to Ø55 mm. The cooling unit is attached to the induction heater to cool down the coils and the electrical units of the power supply.

Figure 4.1 125 KW 3000 Hz Induction Heater

The cooling unit of the induction heater is composed of two separate circulating cooling systems. First one is a closed circulating cooling system. Distilled water is used in this system as the cooling fluid for cooling the electrical part and induction coil box, because of its nonconductive property. Other system uses ordinary tap water for cooling the distilled water. Figure 4.2 represents the schematic view of the cooling system. There is a plate type heat exchanger that is used to transfer heat from distilled water to tap water. Figure 4.3 demonstrates the heat exchanger used in the cooling system of the induction heater. The circulating tap water is cooled by a cooling tower. Figure 4.4 represents the cooling tower of the cooling unit of the induction heater.
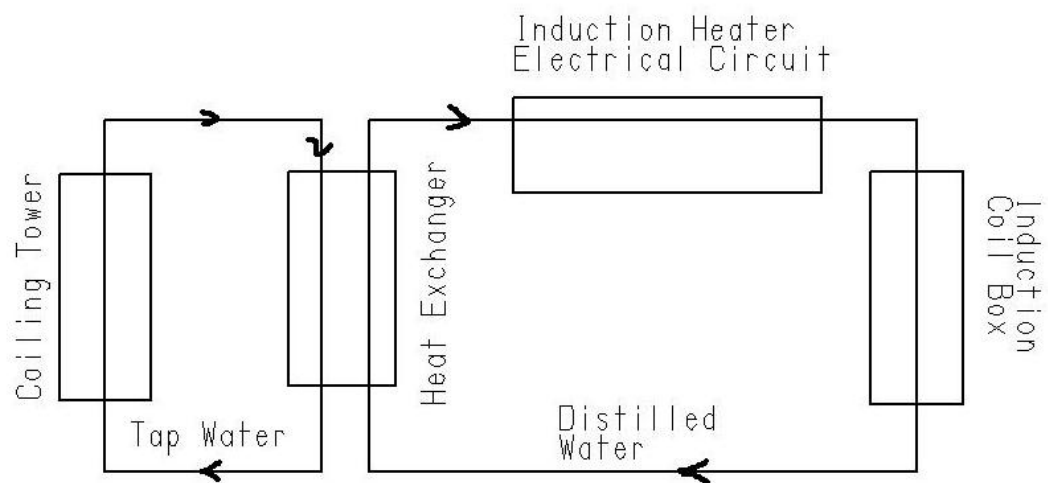
Figure 4.2 Schematic Representation of the Cooling System of the Induction Heater

Figure 4.3 Heat Exchanger of the Cooling Unit

Figure 4.4 Cooling Tower of the Induction Heater Cooling Unit

The induction heater has also workpiece loading system composed of one conveyor and two rotating rollers. The billets that are going to be heated are placed to conveyor and the conveyor carries the billets to the rotating cylinders. The billets are pushed inside the induction coil box with the help of the rotating rollers. Each billet pushes the other one and the movement is achieved by this way. Figure 4.5 and Figure 4.6 demonstrate the workpiece loading system.
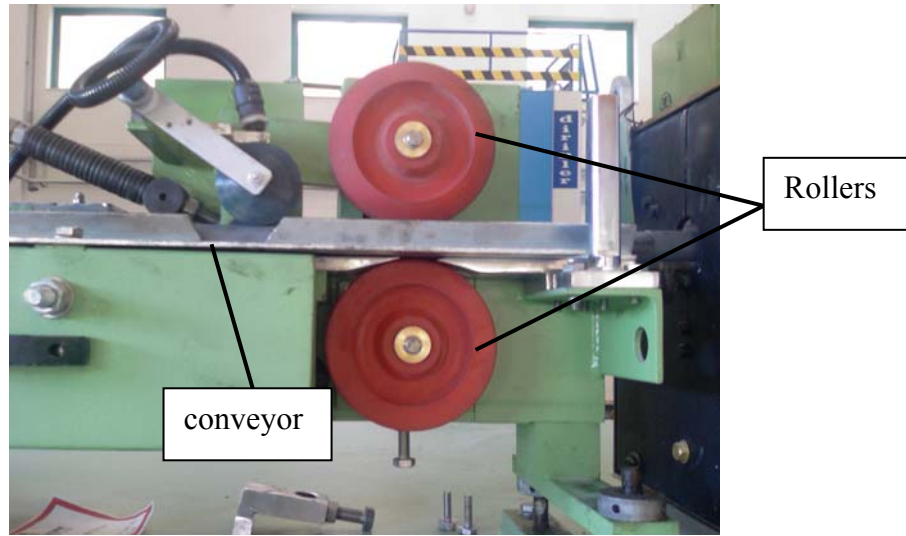
Figure 4.5 Front view of the workpiece loading system (Rotating roller)
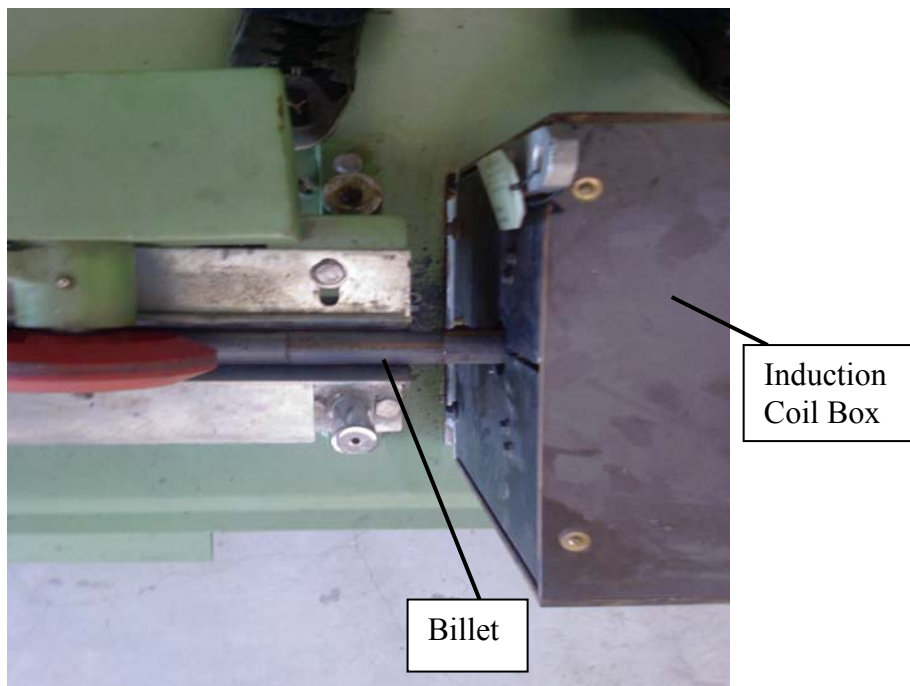
Figure 4.6 Top view of the workpiece loading system (Rotating rollers)

4.2 Induction Coil Boxes

The particular induction heater has three coil boxes with different hole diameters for different billet diameter ranges. Depending on the billet diameter, one of the induction coil box is mounted on the induction heater as shown in Figure 4.7. The first coil box have hole diameter of Ø50 mm and it is recommended by the manufacturer of the induction coil box that this coil box should be worked with the billets having diameters in the range Ø10 mm to Ø30 mm. The second coil box have hole diameter of Ø 70 mm and it is designed for bigger diameter billets, in the range Ø30 mm up to Ø50 mm. The third coil box have hole diameter of Ø 75 mm and heats the billets having diameters of Ø35mm up to Ø55 mm. The three coil boxes are represented in Figure 4.8. The recommended billet diameter range for the corresponding induction coil box is given in Table 4.1.
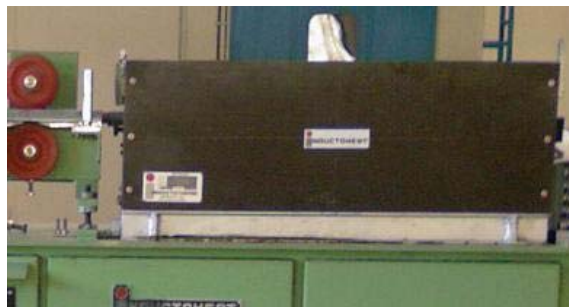
Figure 4.7 Induction coil box mounted on induction heater 125 KW 3000Hz

Figure 4.8 Three induction coil boxes for the 125 KW 3000 Hz induction heaters

Table 4.1 Hole diameters and recommended billet diameter ranges for the induction coil boxes available in METU-BILTIR CENTER

Coil Box No:	Coil Box Hole Diameter (mm)	Recommended Billet Diameters (mm)	
		Minimum Diameter	Maximum Diameter
1	Ø50	Ø10	Ø 30
2	Ø70	Ø30	Ø 50
3	Ø75	Ø35	Ø 55

The billets are carried on a rail inside the induction coil box. The location of rails inside the induction coil boxes are given in the Figure 4.9. As the coil box hole diameter increases the distance between the rails also increases.
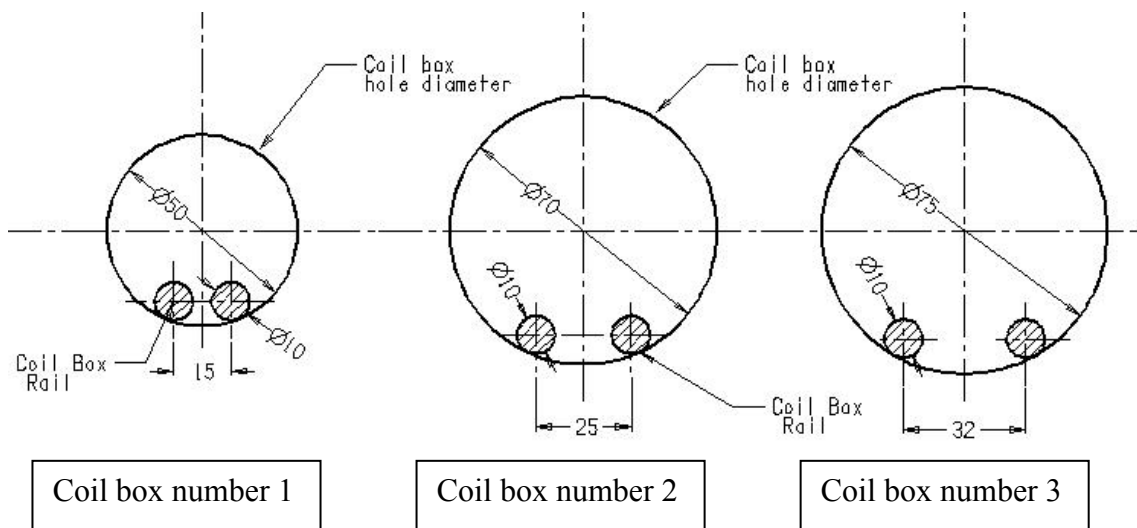
Figure 4.9 Location of Rails in Induction Coil Boxes

4.3 Pyrometer

The temperatures of the heated billets are measured by using optical pyrometer. The RAYTEK Marathon Series MR1SASF type pyrometer is used in the experiments. The pyrometer works with 24 volt power supply. The measurement range of the device is between 600 C^o and 1400 C^o. Figure 4.10 illustrates the pyrometer used in the experiments. The detailed technical specifications of the pyrometer are given in Appendix A.

Figure 4.10 Raytek marathon series MR1SASF model optical pyrometer

4.4 Selection of Test Specimen

The test specimen billets are selected as circular cross-section which is generally used as raw material in hot forging process. The forging billets dimensions are determined according to the geometry of the desired final product. Figure 4.11 demonstrates the forging stages of a sample part.
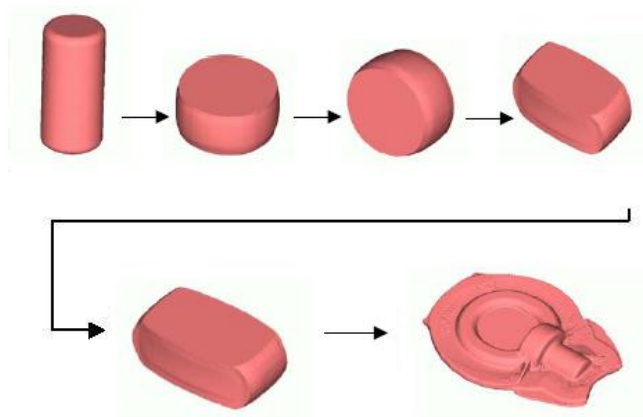
Figure 4.11 Forging Stages of a Sample Part [12]

The billet dimensions are calculated according to the volume of final product. Beginning with the final product volume and adding the scale allowance and flash losses, the required billet volume will be calculated. According to this volume, the billet cross-section can be determined from available raw materials in the market. Generally billets are produced in circular cross-section or square cross-section. The circular cross-section is preferred for axi-symmetric parts.

The induction heater coil box hole diameter is one of the constrain during the determination of the billet cross-section. Since the clearance between coils box hole diameter and billet diameter significantly affects the heating efficiency, it is recommended to choose a billet diameter as close as to the available induction coil box hole diameters, or to use induction heater coil box with a hole diameter as close as to billet diameter.

Several forging parts have been examined in Aksan Steel Forging Company located in Ankara. Choosing the billet diameter of Ø30 mm comes out as the most reasonable by considering the capacity of the 1000 tons forging press. The billet diameter of Ø30 mm can also give opportunity to compare the heating efficiency of the coil box no 1 (Ø10mm- Ø30mm) with the efficiency of the coil box no 2 (Ø30mm- Ø50mm). Then the test specimen is selected as circular cross-section with diameter of Ø30 mm.

The length of test specimen is not critical for the induction heater since the induction furnace is working with fully loaded coil. The feeding system of the induction coil, as illustrated previously in Figure 4.5 and Figure 4.6, is designed such that billets are pushed into the coil. Inside the coil, each billet pushes the other one and by this way movement of the billets is achieved. Therefore in every instance the coil must be fully loaded.

Considering the currently produced parts by using 1000 tons forging press in Aksan Steel Forging Company, the average length of specimen appears around the 100 mm. Therefore, the test specimen length is selected as 100 mm. Since the induction coil box has length of 1000 mm, the coil box will be fully loaded by 10 billets. This length is also convenient for the operator to handle the workpiece. The dimensions of the test specimen are shown in the Figure 4.12.

The billet material has been selected as AISI 1045 since one of the most commonly used material in the forging industry. The material properties of the AISI 1045 are given in Appendix B. The test specimens have been cut by using the sawing machine available in METU-BILTIR CENTER. The positions of test specimens in two different coil boxes are shown in Figure 4.13.
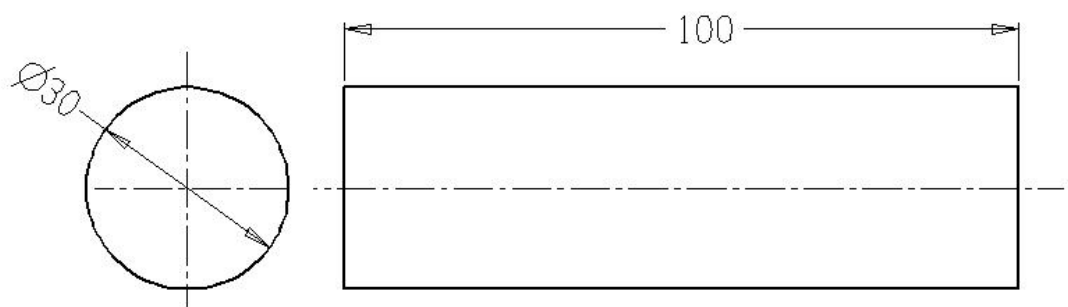
Figure 4.12 Technical drawing of the test specimen (dimensions are in mm)

| First coil (Ø10mm- Ø30mm) | Second coil (Ø30mm- Ø50mm) |
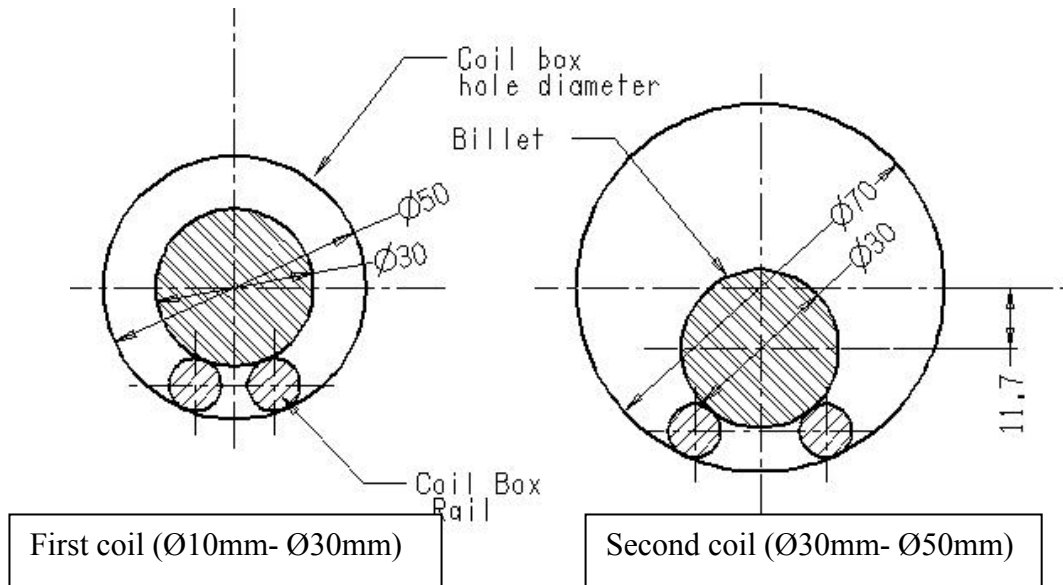
Figure 4.13 Schematic representations of test specimen positions in selected coil boxes

4.5 Determination of Experiment Parameters

The temperature of the heated billet is controlled by using power adjusting button and the conveyor speed adjusting button on the control panel of the induction heater. The power button controls the amount of current provided to the induction coil. The electrical energy is transformed into heating energy inside the billet by the help of induction coil box. Therefore heating power is controlled by power adjusting button. Another control button is the conveyor speed adjusting button on the control panel. As it is explained earlier, the billets are pushed into coil box by two rotating roller (Figures 4.5-4.6). The rotating speed of these rollers controls the moving speed of billets. The moving speed of billet is named as "conveyor speed" in this thesis. Figure 4.14 demonstrates the control panel and the power, conveyor speed adjusting buttons   of the induction heater.

Figure 4.14 A view of control panel of the induction heater

The power level and the conveyor speed level on the adjusting button and corresponding real values are tabulated in Table 4.2 and Table 4.3. The conveyor speed level on control button versus corresponding speed is plotted on Figure 4.15.

Table 4.2 Power level on control button and corresponding power values

Power Level on the Adjusting Button	Corresponding Power (KW)
0.00	0.00
1.00	12.5
2.00	25.0
3.00	37.5
4.00	50.0
5.00	62.5
6.00	75.0
7.00	87.5
8.00	100.0
9.00	112.5
10.00	125.0

Table 4.3 Conveyor speed level on control button and corresponding speed values

Conveyor Speed Level on the Adjusting Button	Corresponding Speed (mm/s)
0.00	0.00
0.50	2.20
1.00	4.10
1.50	6.00
2.00	7.75
2.50	9.60
3.00	11.33
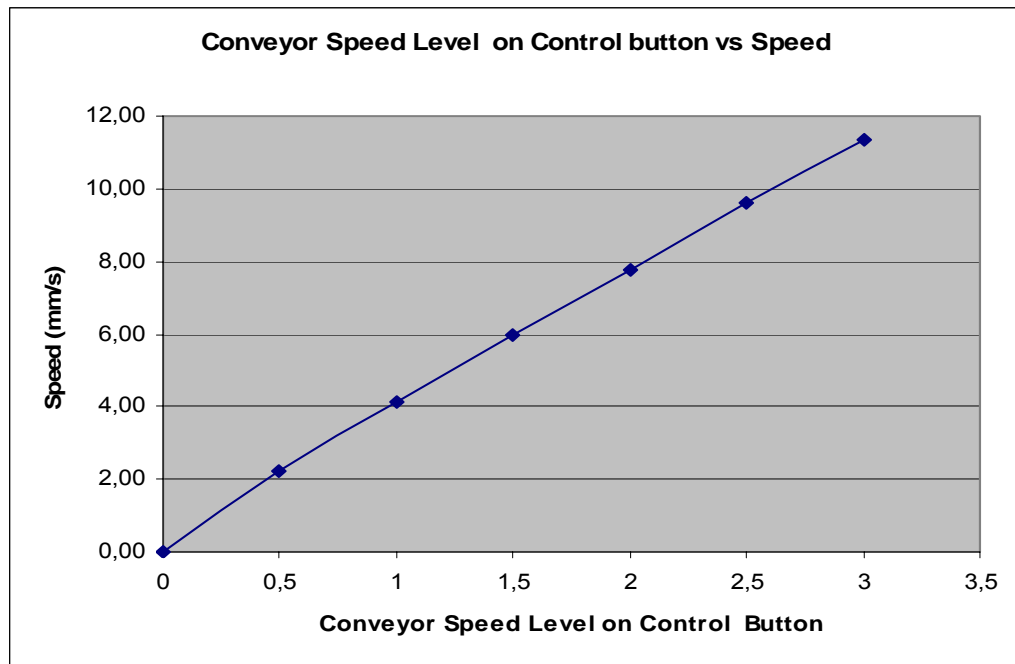
Figure 4.15 Conveyor Speed Level on Control Button versus Corresponding Speed

In addition to power control and conveyor speed control, the induction coil box hole diameter is the other controlling parameter of the temperature of the heated billet. These three factors have been chosen for three experimental factors which are required for the 2^3 factorial design of experiment method it is described in Chapter 3.

4.6 Experimental Procedure

The power level and the conveyor speed level of the induction heater must be set. Before starting the heating, cooling system of the induction heater has to be turned on. It is waited for reaching to the steady state heating condition of the induction heater before the specimens are loaded on the conveyor of the induction heater. The 10 billets have been loaded on the conveyor to be heated with the defined heating parameters. Some dummy billets are required to be loaded behind these test specimens, since as explained in Section 4.1, the movement of the billets to be heated can be achieved by pushing each billet by the billet behind this particular billet. After test specimens had been heated, the temperatures of the billets were measured by using the optical pyrometer and recorded in a table. The operation steps during each set of experiment are given in Figure 4.16.
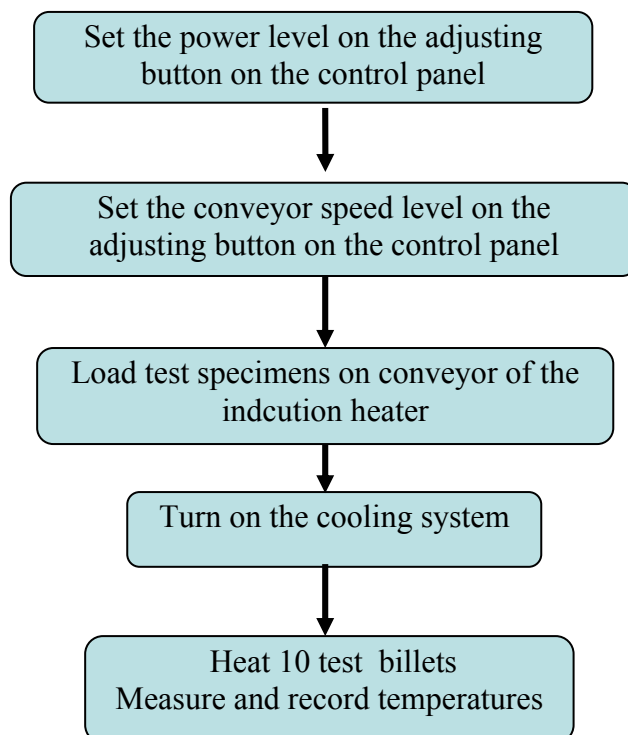
Figure 4.16 Flowchart of Operation Steps for Each Set of Heating Experiment

These operation steps for the heating experiments have been repeated 40 times in four main groups of experiments by using 400 test specimens. These test groups are given in Table 4.4.

In test group A, experiments have been performed to find out effect of the power on the resultant temperature of the heated billet. The upper and the lower limiting values of power, that are required for the 2^3 factorial design of experiments for the induction heating, have been determined in this group of experiments. This test group includes 11 different sets of experiments as described in Section 4.6.1.

In test group B, in a similar way with the test group A, experiments have been performed to find out the upper and the lower limiting values of the conveyor speed that are required for the 2^3 factorial design of experiments for the induction heating. 12 different sets of experiments in the test group B, have been realized as described in Section 4.6.2

In test group C, the 2^3 factorial experiments for the induction heating have been performed. For the 2^3 factorial design of experiments, 8 different sets of experiment have been performed. For each set of experiment, 10 different billets have been heated and the temperatures have been recorded. The test group C will be described in Section 5.1.

In test group D, 9 set of experiments have been performed to verify the mathematical formula derived by using results of the 2^3 factorial experiments which will be described in Section 5.4.

Table 4.4 Experiments performed for induction heating

Test Group	Purpose
Test Group A	Power range determination experiments
Test Group B	Conveyor Speed Range determination experiments
Test Group C	2^3 Factorial Experiments
Test Group D	Verification experiments for the mathematical formula for prediction of heated billet temperature

4.6.1 Determination of the Power Range

Test group A experiments have been performed to find out effect of the power on the resultant temperature of the heated billet. Starting from lowest level, power level has been increased in each experiment up to achieve the upper limit of the hot forging temperature which is considered as about 1300 $^{\circ}$C. During these experiments, the conveyor speed level has been kept constant. The similar experiments are performed with changing the coil box. Temperature measurements have been realized on 10 billets for each set of parameters. The average temperatures of the heated billets are given in the Table 4.5. The average resultant temperatures of the heated billets are plotted against the changing power values in Figure 4.17.

Table 4.5 Experiments Performed for Determination of Power Level

Experiment number	Power KW	Conveyor Speed mm/s	Coil Box Hole Diameter mm	Average Billet Temperature $^{\circ}$C
A-1	25.0	4.10	Ø 70	721
A-2	37.5	4.10	Ø 70	746
A-3	50.0	4.10	Ø 70	863
A-4	62.5	4.10	Ø 70	982
A-5	75.0	4.10	Ø 70	1063
A-6	87.5	4.10	Ø 70	1197
A-7	100.0	4.10	Ø 70	1251
A-8	25.0	4.10	Ø 50	777
A-9	37.5	4.10	Ø 50	998
A-10	50.0	4.10	Ø 50	1161
A-11	62.5	4.10	Ø 50	1300
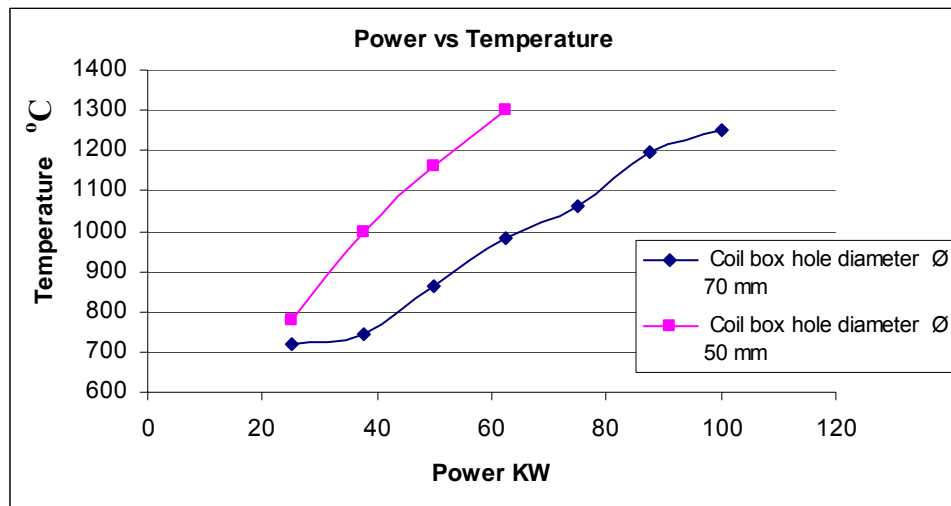
Figure 4.17 Temperature Distributions against the Power Level

The experiments performed for the determination of the power range show that the upper limit of the power level is 62.5 KW, since after that point the temperature for the induction coil box with hole diameter Ø 50 mm goes above 1300 $^{\circ}$C that is over the limit temperature for the steel forging billet. The lower limit is selected as 25.0 KW as level "2" on the power control button. Then the limits of the power level have been set.

4.6.2 Determination of the Conveyor Speed Range

The test group B experiments have been performed to investigate effect of the conveyor speed on the resultant temperature of the heated billet. The power and the coil box hole diameter have been kept constant and the conveyor speed has been changed. In a similar way with previous experiments, 10 billets have been heated and the temperatures have been measured for each case. The experiments have been repeated for different power values as well. The averages of the measured temperatures are tabulated in Table 4.6.

Table 4.6 Experiments Performed for Determination of Conveyor Speed Level

Experiment number	Power KW	Conveyor Speed mm/s	Coil Diameter mm	Average Temperature ^{o}C
B-1	100.0	4.10	Ø 70	1251
B-2	100.0	6.00	Ø 70	1154
B-3	100.0	7.75	Ø 70	1088
B-4	100.0	9.60	Ø 70	1066
B-5	87.5	4.10	Ø 70	1197
B-6	87.5	6.00	Ø 70	1137
B-7	87.5	7.75	Ø 70	1071
B-8	87.5	9.60	Ø 70	1048
B-9	75.0	4.10	Ø 70	1063
B-10	75.0	6.00	Ø 70	1043
B-11	75.0	7.75	Ø 70	990
B-12	75.0	9.60	Ø 70	941
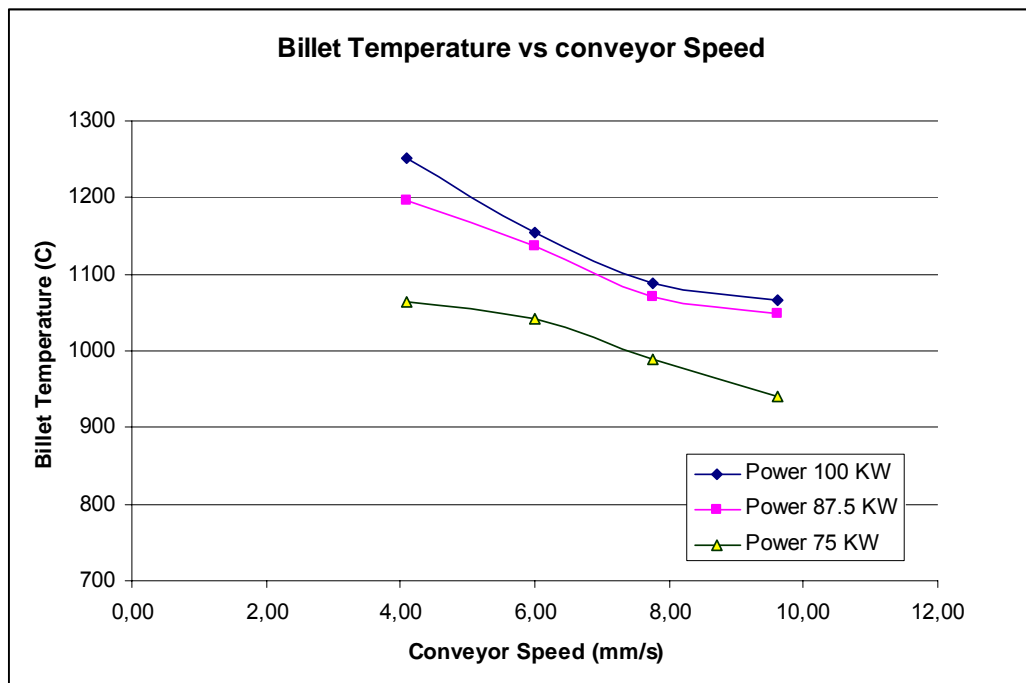
Figure 4.18 Temperature Distributions against the Conveyor Speed Level for Coil Box Hole Diameter of Ø 70mm

Figure 4.18 demonstrates the effect of changing conveyor speed on the heated billet temperature for different power values and for a certain coil box hole diameter. The resultant average temperatures of the heated billets that are given in Table 4.6 and Figure 4.18 show that as the conveyor speed increases, the temperature of the heated billet decreases. The decreasing trend of the temperature is similar for the three different power values.

The experiments for the determination of conveyor speed using different power levels has pointed out that, the conveyor speed 9.60 mm/s can be taken as the higher limit of the conveyor speed value, since even for the highest value of power (i.e. 100 KW) the temperature of the heated billets drops to lower limits of hot forging temperatures. Therefore, considering the temperature drop for lower power values, the upper limit of the conveyor speed has been selected as 9.60 mm/s. It should be also noted that this conveyor speed corresponds to a heating time of about 10 sec/part. Increasing the conveyor speed will reduce the heating time. A heating time which is less than 10 sec/part is not practical if the cycle time of forging process is considered.

In a similar way, the conveyor speed 4.10 mm/s has been selected as the lowest limit of the conveyor speed. Since the temperature of the heated billet will go beyond the upper limit of hot forging steel billet temperature (i.e.1300 ^{o}C) for the lower conveyor speed than the 4.10 mm/s. A conveyor speed of 4.10 mm/s corresponds to a heating time of about 25 sec/part. Decreasing the conveyor speed will increase the heating time and it may cause reducing the productivity. Therefore, the lower limit of the conveyor speed has been selected as 4.10 mm/s.

CHAPTER 5

EXPERIMENTAL RESULTS AND TEMPERATURE PREDICTION FORMULA

In this experimental study, power, conveyor speed and coil box hole diameter have been chosen as induction heating parameters (i.e. factors) affecting heating process of the billets. The resultant temperature of heated billet has been also chosen as the objective output parameter of the heating process. Design of Experiment Method with 2^3 Factorial Design has been used to plan and execute the experiments as described in Chapter 3.

As described in Chapter 4, the 8 different sets of experiments have been performed by setting the factors to the lower and the higher values in a combination. For each set of experiments, 10 billets have been heated and temperatures have been measured and recorded. The average temperatures of each of these 10 measurements have been used in calculations of the main and the interaction effects of these three factors according to Design of Experiment Method. The mathematical formula for the prediction of resultant temperature of the heated billet has been derived by using linear Regression Method as described in Chapter 3. The derived formula has been examined to be verified by applying other sets of heating parameters that are both in and the out of the selected range of parameters.

5.1 2^3 Factorial Experiments for Induction Heating

According to the 2^3 Factorial Design of Experiment Method, the factors that are power, conveyor speed and coil box hole diameter have two levels: high and low level. The levels of these factors that are used in the experiments tabulated in Table 5.1.

Table 5.1 Experimental Parameters and their Limits

Heating Parameters	Low	High
Power Level	25 (KW)	62.5 (KW)
Conveyor Speed Level	4.10 (mm/s)	9.60 (mm/s)
Coil Box Hole Diameter	Ø 50 mm	Ø 70 mm

The geometric representation of the 2^3 factorial design for induction heating of billets and the levels of the factors are shown in Figure 5.1.
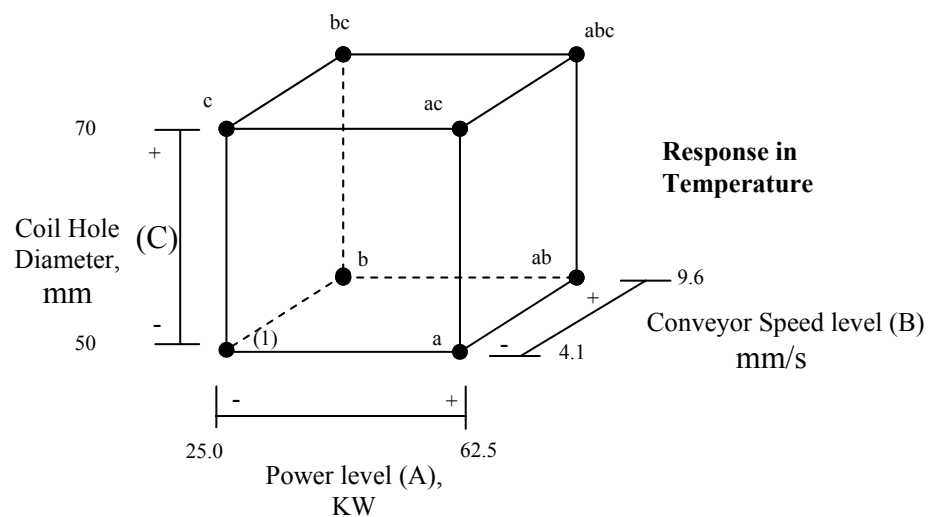
Figure 5.1   Geometrical Representation of the 2^3 Factorial Design for Induction Heating Experiments

The experiments have been conducted by applying different levels of factors as it is demonstrated in Figure 5.1. For each set of factors, 10 different billets have been heated and the temperatures of the heated billets have been measured and recorded. Figure 5.2 shows some billets that are heated during the experiments. The factor levels and the measured resultant temperatures of the heated billets are tabulated in Table 5.2.

Figure 5.2 Heated billets during the experiments

.

Table 5.2 Results of 2^3 Factorial Induction Heating Experiments

| Experiment No | Designation in Design of Experiment | Input Parameter Values | | | Response of the experiments | | | | | | | | | | | Average Temp. °C |
| | | Power KW | Conveyor Speed mm/s | Coil Box Hole Diameter mm | Measured Temperature of the 10 Billets °C | | | | | | | | | | |
					1	2	3	4	5	6	7	8	9	10	
C-1	1	25.0	4.10	Ø 50	775	779	778	760	774	786	790	772	779	778	777
C-2	a	62.5	4.10	Ø 50	1290	1310	1285	1314	1305	1295	1289	1293	1299	1315	1300
C-3	b	25.0	9.60	Ø 50	720	728	726	729	727	715	719	728	718	726	724
C-4	ab	62.5	9.60	Ø 50	1158	1136	1149	1153	1145	1137	1141	1143	1148	1155	1147
C-5	c	25.0	4.10	Ø 70	725	717	720	728	726	718	715	716	724	719	721
C-6	ac	62.5	4.10	Ø 70	978	986	975	980	983	990	985	976	979	986	982
C-7	bc	25.0	9.60	Ø 70	650	654	662	652	648	655	640	644	652	649	652
C-8	abc	62.5	9.60	Ø 70	892	880	878	884	883	898	876	889	885	886	886

5.2   Effect Estimation

Equations 3.1-3.10 have been used to calculate the main and interaction effects of the selected parameters. Since the average values are used, n is taken as one in the equations.

By using Equation 3.1, the main effect of the Power which is designated as "A", can be calculated as follows;

$$A = \frac{1}{4}[1300 - 777 + 1147 - 724 + 982 - 721 + 886 - 652]$$
$$A = \frac{1}{4}[1441] = 360.25$$

(5.1)

By using Equation 3.2, the main effect of the Conveyor Speed which is designated as "B", can be calculated as follows;

$$B = \frac{1}{4}[724 - 777 + 1147 - 1300 + 652 - 721 + 886 - 982]$$
$$B = \frac{1}{4}[-371] = -92.75$$

(5.2)

By using Equation 3.3, the main effect of the Coil Box Hole Diameter which is designated as "C", can be calculated as follows;

$$C = \frac{1}{4}[721 - 777 + 982 - 1300 + 652 - 724 + 886 - 1147]$$
$$C = \frac{1}{4}[-707] = -176.75$$

(5.3)

By using Equation 3.4, the interaction effect of Power with the Conveyor Speed which is designated with "AB", can be calculated as follows;

$$AB = \frac{1}{4}[886 - 652 + 1147 - 724 - 982 + 721 - 1300 + 777]$$
$$AB = \frac{1}{4}[-127] = -31.75$$

(5.4)

By using Equation 3.8, the interaction effect of Power with the Coil Box Hole Diameter which is designated with "AC", can be calculated as follows

$$AC = \frac{1}{4}[886 - 652 + 982 - 721 - 1147 + 724 - 1300 + 777]$$

$$AC = \frac{1}{4}[-451] = -112.75$$

(5.5)

By using Equation 3.9, the interaction effect of Conveyor Speed with the Coil Box Hole Diameter which is designated with "BC", can be calculated as follows;

$$BC = \frac{1}{4}[886 - 982 + 652 - 721 - 1147 + 1300 - 724 + 777]$$

$$BC = \frac{1}{4}[41] = 10.25$$

(5.6)

By using Equation 3.10, the interaction effect of three factors Power, Conveyor Speed and Coil Box Hole Diameter which is designated with "ABC", can be calculated as follows;

$$ABC = \frac{1}{4}[886 - 652 - 982 + 721 - 1147 + 724 + 1300 - 777]$$

$$ABC = \frac{1}{4}[73] = 18.25$$

(5.7)

Table 5.3 Main and interaction effects of the induction heating parameters

Effect	Designation	Value of Effect
Power	A	360.25
Conveyor speed	B	-92.75
Coil box hole diameter	C	-176.75
Power*Conveyor speed	AB	-31.75
Power*Coil box hole diameter	AC	-112.75
Conveyor speed* Coil box hole diameter	BC	10.25
Power*conveyor speed*coil box hole diameter	ABC	18.25
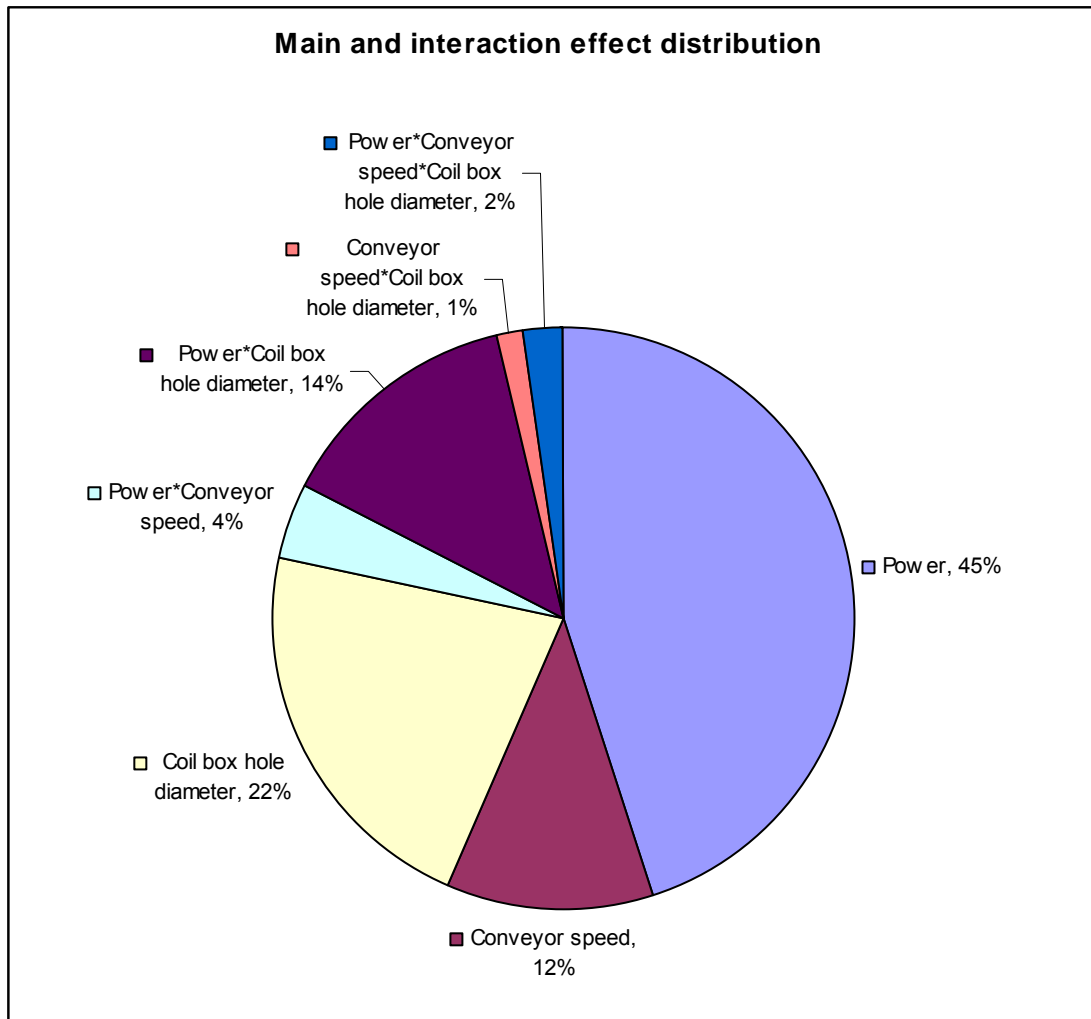
Figure 5.3 Main and interaction effect distribution

Main and interaction effects values are given in Table 5.3. The percentage distribution is represented in Figure 5.3. When their absolute values are compared, the power (A) has the greatest effect on the temperature of the heated billet. The main effect of the coil box hole diameter (C) is in second place and the interaction effect of power and the coil box hole diameter (AC) is in the third place. The main effect conveyor speed (B) level is in fourth place and it is still considerable. The others main and the interaction effects are negligible compared total effects.

The same calculations can also be done by using a commercially available statistical analysis software MINITAB [22]. The output of the MINITAB software is given in Appendix C. The main and the interaction effects plots obtained from MINITAB software are given in Figure 5.4 and Figure 5.5.
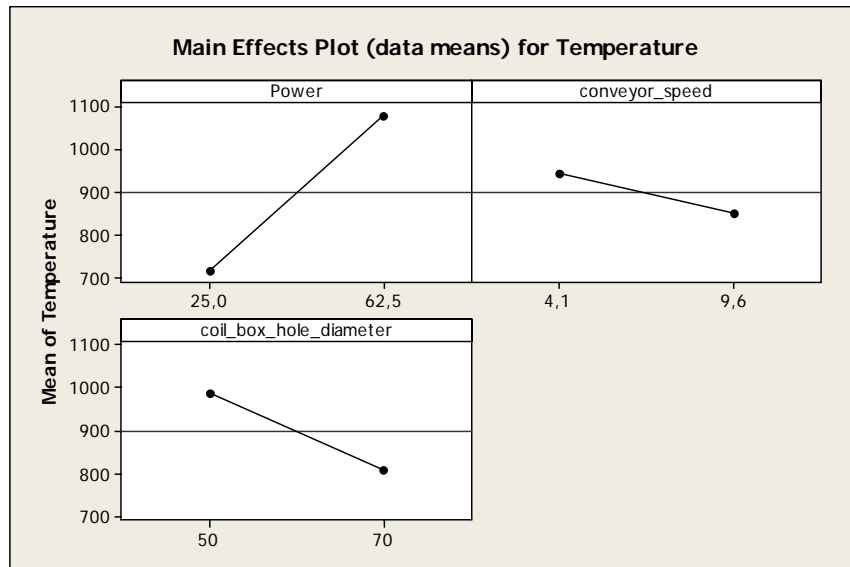
Figure 5.4 Main Effect Plots
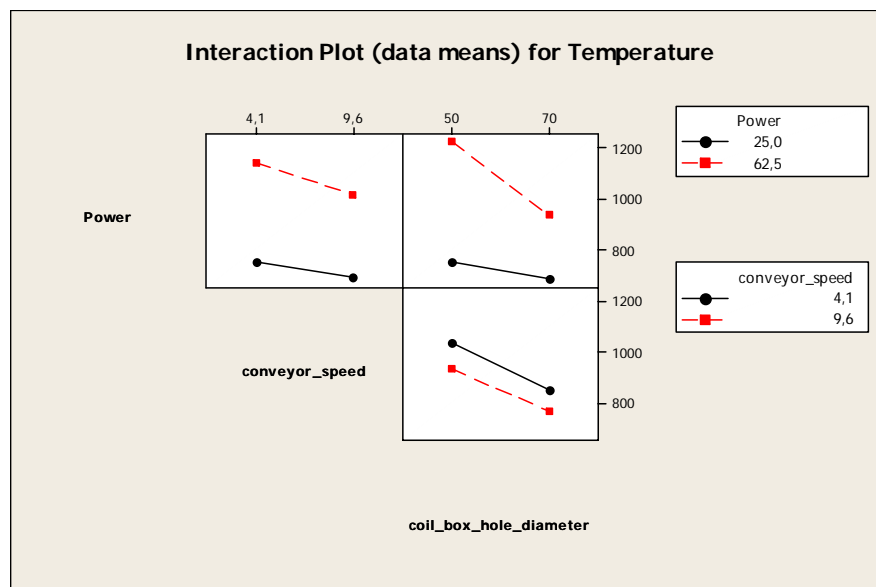
Figure 5.5 Interaction Effect Plots

5.3 Derivation of Temperature Prediction Formula

In order to derive temperature prediction formula, the values of the variable coefficients (β) of the multiple linear regression model, which is described in Chapter 3, have to be calculated. The Least square method is used to compute the β values.

β is determined as fallows;

$$\beta = (X^T \cdot X)^{-1} \cdot (X^T \cdot T) \qquad (5.8)$$

Where X is the matrix obtained from input factors used in the experiments and T is the matrix of results of the experiments (i.e. average temperature values). The input parameters of the experiments and the results of the experiments that are present in Table 5.2 have been used to from the matrices. The matrix X is given as follows. First column is composed of 1, second column is first factor "Power" values in the same order of experiments. Third column is composed of "conveyors speed" values and fourth column is composed of "coil box hole diameters".

$$
X = \begin{pmatrix}
1 & 25 & 4.1 & 50 & 102.5 & 1.25 \times 10^3 & 205 & 5.125 \times 10^3 \\
1 & 62.5 & 4.1 & 50 & 256.25 & 3.125 \times 10^3 & 205 & 1.281 \times 10^4 \\
1 & 25 & 9.6 & 50 & 240 & 1.25 \times 10^3 & 480 & 1.2 \times 10^4 \\
1 & 62.5 & 9.6 & 50 & 600 & 3.125 \times 10^3 & 480 & 3 \times 10^4 \\
1 & 25 & 4.1 & 70 & 102.5 & 1.75 \times 10^3 & 287 & 7.175 \times 10^3 \\
1 & 62.5 & 4.1 & 70 & 256.25 & 4.375 \times 10^3 & 287 & 1.794 \times 10^4 \\
1 & 25 & 9.6 & 70 & 240 & 1.75 \times 10^3 & 672 & 1.68 \times 10^4 \\
1 & 62.5 & 9.6 & 70 & 600 & 4.375 \times 10^3 & 672 & 4.2 \times 10^4
\end{pmatrix} \qquad (5.9)
$$

The temperature matrix is given as follows as in thee same order with experiments;

$$
\text{Temperature} = \begin{pmatrix}
777 \\
1.3 \times 10^3 \\
724 \\
1.147 \times 10^3 \\
721 \\
982 \\
652 \\
886
\end{pmatrix}
\tag{5.10}
$$

The $X^T X$ matrix is

$$
X^T \cdot X = \begin{pmatrix}
8 & 350 & 54.8 & 480 & 2.397 \times 10^3 & 2.1 \times 10^4 & 3.288 \times 10^3 & 1.438 \times 10^5 \\
350 & 1.813 \times 10^4 & 2.397 \times 10^3 & 2.1 \times 10^4 & 1.242 \times 10^5 & 1.087 \times 10^6 & 1.438 \times 10^5 & 7.449 \times 10^6 \\
54.8 & 2.397 \times 10^3 & 435.88 & 3.288 \times 10^3 & 1.907 \times 10^4 & 1.438 \times 10^5 & 2.615 \times 10^4 & 1.144 \times 10^6 \\
480 & 2.1 \times 10^4 & 3.288 \times 10^3 & 2.96 \times 10^4 & 1.438 \times 10^5 & 1.295 \times 10^6 & 2.028 \times 10^5 & 8.871 \times 10^6 \\
2.397 \times 10^3 & 1.242 \times 10^5 & 1.907 \times 10^4 & 1.438 \times 10^5 & 9.875 \times 10^5 & 7.449 \times 10^6 & 1.144 \times 10^6 & 5.925 \times 10^7 \\
2.1 \times 10^4 & 1.087 \times 10^6 & 1.438 \times 10^5 & 1.295 \times 10^6 & 7.449 \times 10^6 & 6.706 \times 10^7 & 8.871 \times 10^6 & 4.594 \times 10^8 \\
3.288 \times 10^3 & 1.438 \times 10^5 & 2.615 \times 10^4 & 2.028 \times 10^5 & 1.144 \times 10^6 & 8.871 \times 10^6 & 1.613 \times 10^6 & 7.056 \times 10^7 \\
1.438 \times 10^5 & 7.449 \times 10^6 & 1.144 \times 10^6 & 8.871 \times 10^6 & 5.925 \times 10^7 & 4.594 \times 10^8 & 7.056 \times 10^7 & 3.654 \times 10^9
\end{pmatrix}
\tag{5.11}
$$

The inverse of $X^T X$ matrix is

$$
(X^T \cdot X)^{-1} = \begin{pmatrix}
214.738 & -4.147 & -26.997 & -3.482 & 0.521 & 0.067 & 0.438 & -8.454 \times 10^{-3} \\
-4.147 & 0.095 & 0.521 & 0.067 & -0.012 & -1.537 \times 10^{-3} & -8.454 \times 10^{-3} & 1.932 \times 10^{-4} \\
-26.997 & 0.521 & 3.941 & 0.438 & -0.076 & -8.454 \times 10^{-3} & -0.064 & 1.234 \times 10^{-3} \\
-3.482 & 0.067 & 0.438 & 0.058 & -8.454 \times 10^{-3} & -1.121 \times 10^{-3} & -7.297 \times 10^{-3} & 1.409 \times 10^{-4} \\
0.521 & -0.012 & -0.076 & -8.454 \times 10^{-3} & 1.74 \times 10^{-3} & 1.932 \times 10^{-4} & 1.234 \times 10^{-3} & -2.821 \times 10^{-5} \\
0.067 & -1.537 \times 10^{-3} & -8.454 \times 10^{-3} & -1.121 \times 10^{-3} & 1.932 \times 10^{-4} & 2.562 \times 10^{-5} & 1.409 \times 10^{-4} & -3.221 \times 10^{-6} \\
0.438 & -8.454 \times 10^{-3} & -0.064 & -7.297 \times 10^{-3} & 1.234 \times 10^{-3} & 1.409 \times 10^{-4} & 1.065 \times 10^{-3} & -2.057 \times 10^{-5} \\
-8.454 \times 10^{-3} & 1.932 \times 10^{-4} & 1.234 \times 10^{-3} & 1.409 \times 10^{-4} & -2.821 \times 10^{-5} & -3.221 \times 10^{-6} & -2.057 \times 10^{-5} & 4.702 \times 10^{-7}
\end{pmatrix}
\tag{5.12}
$$

And the X^T Temperature matrix is,

$$X^T \cdot \text{Temperature} = \begin{pmatrix} 7.189 \times 10^3 \\ 3.415 \times 10^5 \\ 4.822 \times 10^4 \\ 4.243 \times 10^5 \\ 2.288 \times 10^6 \\ 2.01 \times 10^7 \\ 2.846 \times 10^6 \\ 1.347 \times 10^8 \end{pmatrix} \tag{5.13}$$

β is determined by using Equation 5.8 as follows;

$$\beta = \begin{pmatrix} 0.964 \\ 37.029 \\ 31.879 \\ 8.344 \\ -1.37 \\ -0.422 \\ -0.588 \\ 0.018 \end{pmatrix} \tag{5.14}$$

As a result of the least square method calculations, the mathematical model for temperature prediction is obtained as follows;

$$\text{T} = 0.964 + 37.029 \cdot P + 31.879 \cdot S_c + 8.344 \cdot D_c - 1.37 \cdot P \cdot S_c$$
$$- 0.422 \cdot P \cdot D_c - 0.588 \cdot S_c \cdot D_c + 0.018 \cdot P \cdot S_c \cdot D_c \tag{5.15}$$

Where,

T : Temperature ($^{\text{o}}$C)

P : Power (KW)

S_c : Conveyor Speed (mm/s)

D_c : Coil Box Hole Diameter (mm)

5.4 Verification Tests

The prediction formula is checked by performing some additional experiments with different heating parameters. The setting values of the factors, the measured temperatures and the predicted temperature of the heated billets are tabulated in the Table 5.4. The difference between the measured and the predicted temperatures and the percentage error are also given in same table.

Table 5.4 The observed temperature values and the predicted temperatures

Exp. No:	Power KW	Conveyor Speed mm/s	Coil Box Diameter mm	Predicted Temp. ^oC	Measured Average Temp. ^oC	Error ^oC	Percentage Error
D-1	100.0	4.10	Ø 70	1250	1251	1	% 0.08
D-2	75.0	7.75	Ø 70	1010	990	20	% 2.00
D-3	87.5	6.00	Ø 70	1126	1137	9	% 0.80
D-4	62.5	4.10	Ø 70	987	982	5	% 0.50
D-5	50.0	4.10	Ø 70	889	863	26	% 3.01
D-6	50.0	6.00	Ø 50	1088	1079	9	% 0.83
D-7	37.5	7.75	Ø 50	898	876	22	% 2.51
D-8	37.5	6.00	Ø 50	925	938	13	% 1.38
D-9	25.0	4.10	Ø 50	779	778	1	% 0.08

The maximum percentage error between the measured temperatures with the predicted temperatures is around the 3 %. This maximum error percentage is in acceptable range. For the experiments D-1, D-2 and D-3 given in Table 5.4, although the heating parameters are out of the range defined in Section 5.1, the predicted and the measured temperatures are quite close to each other. Therefore the temperature prediction formula is found as valid both in the defined limits and out of the defined limits with in the acceptable error range.

CHAPTER 6

CONCLUSIONS AND FUTURE WORK

6.1 Conclusions

In this study, induction heating process has been analyzed for a particular induction heater (125KW 3000Hz) that is available in METU-BILTIR Research and Development Center Forging Laboratory. Initially, the factors affecting the induction heating process have been investigated and three factors have been chosen which are power, conveyor speed and induction coil box hole diameter. The lower and the upper limits of these factors have been determined by performing a series of experiments. After setting limits of the factors, 2^3 Factorial Design of Experiment Method has been performed to find out the relations between these factors and the resultant billet temperature. For each set of factor level, temperature measurements have been done for 10 different heated billets. A mathematical formula has been derived for the prediction of the temperature of the billet to be heated. Finally, verification experiments have been realized to see the validity of the temperature prediction formula.

After performing the 2^3 factorial design of experiments, it has been found that the power is the main factor affecting the resultant temperature of the heated billet. Table 5.3 and Figure 5.3 indicate that, change in the power level results the greatest amount of change in the temperature of the billet compared to the other factors. The main effect of power is the most significant one with the highest percentage of 45 %.

It is also observed that, the main effect of the coil box hole diameter is the second significant factor controlling the temperature of the heated billet. The main effect of the coil box hole diameter has been calculated as 22 %. The increase in the coil box hole diameter results in a decrease in the temperature of the heated billet.

The interaction effect of power and coil box hole diameter is in the third place with the percentage of 14 %. When it is compared with the other interaction effects, the greatest interaction effect is this one.

The conveyor speed level has also considerable effect on the temperature of the heated billet. The conveyor speed effect percentage is 12 %. The increase in the conveyor speed level results in a decrease in the temperature of the heated billet.

The interaction effect of the power and conveyor speed is 4 % and it is relatively small comparing to the other effects.

The percentage of remaining effects is 3 % in total and these effects are negligible compared to the other effects.

Using the 2^3 factorial design of experiments results, it has been derived a temperature prediction formula given by Equation 5.15.

The formula is checked by a set of experiments and the differences between observed and the predicted temperatures have been tabulated previously in Table 5.4. The maximum percentage error is about 3 % and the error is in acceptable range. Therefore, successful correlation between the measured and the predicted temperatures have been observed.

In this study, it is shown that the 2^3 Factorial Design of Experiments combined with method of multiple linear regression can be succesfully applied to derive a mathematical model for prediction of the resultant temperature of the heated billet. The advantage of this method is that the formula may be derived without performing a large number of experiments.

The formula which is derived in this study has been found as valid both in and out of the defined factors ranges.

6.2 Future works

Future works to this study may be listed as fallows:

- A software can be developed to determine the operating parameters of the induction heater for desired temperature of the billet that is to be heated. The derived formula can be used in this software and the software will give optimum operating factors for a desired billet temperature.

- A mathematical model can be establish relating with the operating parameters and the temperature distribution inside the billet for a given geometry and this mathematical model can be used to find out the temperature difference between surface and the core during the heating.

- The experiments can be extended by using different billet material, billet dimensions and coil boxes or different induction heaters with different working frequency. A database for induction heating operating conditions for different materials and induction heaters can be generated.

REFERENCES

[1]   Rudnev, V., Loveless D, Cook R., Black M., *"Handbook of induction heating"*, New York, Marcel Dekker, 2003

[2]   Avitzur, B., *"Handbook of metal-forming processes"*, New York, Chichester,Willey, 1983

[3]   Bruchanow A.N., Rebelski A. W., *"Gesenkschmieden und Warmpresse"*, Verlag Technik, Berlin, 1955

[4]   William H., Hayt Jr., Buck J.A.,   *"Engineering Electro Magnetics",* Mc Graw Hill, New York , 2001

[5]   Chen M., Yuan L., Gan Z., *"Rapid and selective induction heating for sensor packing",* IEEE Transactions on Magnets. 2005

[6]   Erickson, C.J., *"Handbook of electrical heating for industry"*, New York, Institute of Electrical and Electronics Engineers, 1995

[7]   Kawaguchi H., Enokizono M., *"Thermal and magnetic field analysis of induction heating problems"*. Journal of Materials Processing Technology 2005,

[8]   Boadi A., Tsuchida Y., Todaka T., Enokizono M., *"Designing of Suitable Construction of High Frequency Induction Heating Coil by Using Finite element Method"*. IEEE Transactions on Magnets Vol. 41, 2005

[9]   Inan S.U.,Inan S.A., "E*ngineering Electromagnetic"*. Addison Wesley, Melno Park California, 1999

[10]   Montgomery D.C., *"Design and Analysis of Experiments"*, Fifth Edition, New York , Willey, 2001

[11]   İlkgün Ö., *"Effects of Production Parameters on Porosity and Hole Properties in Laser Sintering Rapid Prototyping Process"*, M. S. Thesis, Middle East Technical University, Ankara, Turkey, 2005

[12]   Civelekoglu B., *"Analysis of Forging for Three Diffrent Alloy Steel"*, M. Sc. Thesis, Middle East TechnicalUniversity, Ankara, Turkey, 2003.

[13]   Nerg J., Tolsa K., Silventoien P., Partenen J. *"A Dynamic Model for the Simulation of Induction Heater"* .IEEE Transaction on Magnetics Vol. 35. 1999

[14]   Shen H.., Yao Z.Q., Shi Y.J, Hu J. *"Study on Temperature Field Induced in High Frequency Induction Heating"*. ACTA METALLURCA Vol. 19. 2006

[15]   Jang J.Y, Chiu Y.W., *"Numerical and Experimental Thermal Analysis for a Metallic Hollow Cylinder Subjected to Stepwise Electro-magnetic Induction Heating"*. Applied Thermal Engineering, 2006

[16]   Rudnev V., *"Systematic Analysis of Induction Coil Failures "*. Heat Treating Process, Inductotherm Releases 2007

[17]   Chen S. C., Peng H.S., Chang J. A., Jong W.R., *"Simulations and Verification of Induction Heating on a Mold Plate"*. Int. Comm. Heat Mass Transfer Vol. 31,2004

[18]   Okman O., *"Free Forming of the Locally Heated Specimens"*, M. Sc. Thesis, Middle East Technical University, Ankara, Turkey, 2005

[19]   Çelik K. A., *"Development of a Methodology for Prediction of Surface Roughness of Curved Cavities Manufactured by 5 Axes CNC Milling"*, M. Sc. Thesis, Middle East Technical University, Ankara, Turkey, 2007

[20]   Raytek Marathon Series MR1SASF Optic Pyrometer Operator's Manual, 2006

[21]   Mat Web Material Property Data
       http://www.matweb.com/search/SpecificMaterial.asp?bassnum=M1045J
       Last Access: September 01, 2007

[22]   MINITAB Release 14, Statistical software
        http://www.minitab.com
       Last Access: September 03, 2007

APPENDIX A

TECHNICAL PROPERTIES OF OPTICAL PYROMETER

The technical properties of the optical pyrometer which has been used in the experiments can be summarized as follows. [20]

Model: RAYTEK, Marathon Series MR1SASF

Description: This pyrometer is 2-color, infrared, and noncontact with variable focus. In 2-color mode pyrometers, temperatures are determined from the ratio of the two separate and overlapping infrared bands. The 2 color mode is best for measuring the temperature range of the target that are partially obscured by other objects, openings, screens or viewing windows that reduce energy and by dirt, smoke or steam in the atmosphere. The 2 color mode can also be used on the targets that do not completely fill the measurements spot, provided the background is much cooler than the target.

Temperature Range:

$600C^o$-$1400C^o \pm 1 \ ^oC$

Standard Focus:

44:1

Optical Resolution:

600 mm to ∞

Power supply:

24 V DC

APPENDIX B

MATERIAL PROPERTIES FOR AISI 1045

The properties for AISI 1045 which has been used in experiment are found in web [21].

Subcategory: AISI 1000 Series Steel; Carbon Steel; Ferrous Metal; Medium Carbon Steel; Metal

Composition (%):

C	Fe	Mn	P	S
0.42-0.50	98.51-98.98	0.6-0.9	Max 0.04	Max 0.05

Physical Properties:

Density: 7870 kg/mm^3

Hardness: 170 Brinell

Mechanical Properties at Room Temperature:

Tensile Strength (Ultimate)	: 515 MPa
Yield Strength	: 485 MPa
Shear Modulus	: 90 GPa
Poisson's Ratio	: 0.29
Modulus of Elasticity	: 200 GPa

Thermal Properties:

Specific Heat Capacity	: 486 Joule/Kg-C^o at 100C^o
Thermal conductivity	: 51.9 W/m-K

MINITAB OUTPUT FOR THE DESING OF EXPERIMENT

MINITAB [22] software has been used for the 2^3 Design of Experiments to calculate main and the interaction effects. The output of the program is given as follows

Full Factorial Design

```
Factors:    3   Base Design:         3; 8
Runs:      80   Replicates:          10
Blocks:     1   Center pts (total):   0


All terms are free from aliasing.
```

Factorial Fit: Temperature versus Power; conveyor_speed; coil_box_hol

```
Estimated Effects and Coefficients for Temperature (coded units)

Term                         Effect    Coef  SE Coef       T      P
Constant                             898,63    2,211  406,35  0,000
Power                        360,25  180,12    2,211   81,45  0,000
conveyor_speed               -92,75  -46,37    2,211  -20,97  0,000
coil_box_hole_diameter      -176,75  -88,37    2,211  -39,96  0,000
Power*conveyor_speed         -31,75  -15,87    2,211   -7,18  0,000
Power*coil_box_hole_diameter -112,75 -56,37    2,211  -25,49  0,000
conveyor_speed*               10,25    5,12    2,211    2,32  0,049
  coil_box_hole_diameter
Power*conveyor_speed*         18,25    9,13    2,211    4,13  0,003
  coil_box_hole_diameter


S = 8,84590   R-Sq = 99,91%   R-Sq(adj) = 99,84%


Analysis of Variance for Temperature (coded units)

Source             DF  Seq SS  Adj SS  Adj MS        F      P
Main Effects        3  678493  678493  226164  2890,28  0,000
2-Way Interactions  3   55303   55303   18434   235,58  0,000
3-Way Interactions  1    1332    1332    1332    17,03  0,003
Residual Error      8     626     626      78
  Pure Error        8     626     626      78
Total              15  735754
```

```
Estimated Coefficients for Temperature using data in uncoded units

Term                              Coef
Constant                        0,9636
Power                          37,0291
conveyor_speed                 31,8788
coil_box_hole_diameter         8,34364
Power*conveyor_speed           -1,36970
Power*coil_box_hole_diameter   -0,421891
conveyor_speed*                -0,587879
  coil_box_hole_diameter
Power*conveyor_speed*          0,0176970
  coil_box_hole_diameter


Alias Structure
I
Power
conveyor_speed
coil_box_hole_diameter
Power*conveyor_speed
Power*coil_box_hole_diameter
conveyor_speed*coil_box_hole_diameter
Power*conveyor_speed*coil_box_hole_diameter
```

ANOVA: Temperature versus Power; conveyor_speed; coil_box_hole_diameter

```
Factor                  Type   Levels  Values
Power                   fixed       2  25,0; 62,5
conveyor_speed          fixed       2  4,1; 9,6
coil_box_hole_diameter  fixed       2  50; 70


Analysis of Variance for Temperature

Source                       DF      SS      MS       F      P
Power                         1  519120  519120  6634,12  0,000
conveyor_speed                1   34410   34410   439,75  0,000
coil_box_hole_diameter        1  124962  124962  1596,96  0,000
Power*conveyor_speed          1    4032    4032    51,53  0,000
Power*coil_box_hole_diameter  1   50850   50850   649,84  0,000
conveyor_speed*               1     420     420     5,37  0,049
  coil_box_hole_diameter
Power*conveyor_speed*         1    1332    1332    17,03  0,003
  coil_box_hole_diameter
Error                         8     626      78
Total                        15  735754


S = 8,84590   R-Sq = 99,91%   R-Sq(adj) = 99,84%
```